APPLICATION OF RADIOMETRIC METHOD TO DETERMINE RADIOGENIC HEAT AROUND RAFIN REWA HOT SPRING, LERE, KADUNA STATE, NIGERIA

BY

Ibrahim Tijjani BRAJA

DEPARTMENT OF PHYSICS,
FACULTY OF PHYSICAL SCIENCE,
AHMADU BELLO UNIVERSITY, ZARIA
NIGERIA.

MAY, 2018

APPLICATION OF RADIOMETRIC METHOD TO DETERMINE RADIOGENIC HEAT AROUND RAFIN REWA HOT SPRING, DAN-ALHAJI, LERE, KADUNA STATE, NIGERIA

By

IBRAHIM TIJJANI BRAJI, B.Sc. Physics (KUST), 2012

(P14SCPY8033)

BEING A DISSERTIFICATION SUBMITTED TO THE SCHOOL OF POSTGRADUATE STUDIES, AHMADU BELLO UNIVERSITY, ZARIA IN PARTIAL FULFILLMENT OF THE REQUIREMENT FOR THE AWARD OF A MASTER OF SCIENCE DEGREE IN APPLIED GEOPHYSICS.

DEPARTMENT OF PHYSICS,
FACULTY OF PHYSICAL SCIENCE,
AHMADU BELLO UNIVERSITY, ZARIA
NIGERIA.

MAY, 2018

DECLARATION

I declare that the work title "APPLICATION OF RADIOMETRIC METHOD TO DETERMINE RADIOGENIC HEAT AROUND RAFIN REWA HOT SPRING, DAN-ALHAJI, LERE, KADUNA STATE, NIGERIA" has been carried out by me in the Department of Physics under the supervision of Dr. Aminu Ahmed Lawal and Prof. B.B.M Dewu The information derived from the literature has been duly acknowledged in the text and a list of references provided. No part of this research was previously presented for another degree or diploma at this or any other Institution.

Ibrahim Tijjani BRAJI		
Name of Student	Signature	Date

CERTIFICATION

This thesis titled "APPLICATION OF RADIOMETRIC METHOD TO DETERMINE RADIOGENIC HEAT AROUND RAFIN REWA HOT SPRING, DAN-ALHAJI, LERE, KADUNA STATE, NIGERIA" meets the regulations governing the award of the Degree of Master of Science in Applied Geophysics of Ahmadu Bello University, Zaria and is approved for its contribution to knowledge and literary presentation.

Dr. Aminu Lawal Ahmad		
Chairman, Supervisory Committee	Signature	Date
Prof. B.B.M Dewu		
Member, Supervisory Committee	Signature	Date
Prof. Rabiu Nasiru		
Ag. Head of Department	Signature	Date
Prof. A.Z. Abubakar		
Dean School of Postgraduate	Signature	Date

DEDICATION

I dedicated this research work to my first family Hajiya Hadiza T. Braji (mama), Hajiya Aiza T. Braji (baaba), Alhaji Tijjani Braji, Fatima(ummiya), Zainab, Khadija(mami), Muhd (Baba), Hajja O, Biyoni, Abba bossa, Sadiq, Hajjaju, Abdullahi Sir, Mufeedah, Hajiya Hauwa, Khadijanjan And my wife Maryam Rabiu Yadudu.

ACKNOWLEDGEMENT

I am indeed very grateful to Allah (S.W.T) for his guidance, sustenance, strength and protection in the course of this research work and during the entire period of my study (master's program). All glory and honour be unto his holy names.

My profound gratitude goes to my Supervisors, Dr. A. Aminu Lawal and Prof. B.B.M Dewu for their technical guidance, constructive comments and advices.

My heartfelt appreciation also goes to the Head of Department (H.O.D) Physics, late Prof. Y.I. Zakari, Ag. Head of Department Prof. Rabiu Nasiru, Postgraduate coordinator, Dr. N.N. Garba, Coordinator Applied Geophysics unit, Dr. A.L. Aminu, Seminar coordinator, Dr. M.A. Onoja, and Technical staff of Physics department, Ahmadu Bello University, Zaria for their efforts in ensuring a successful running of the M.Sc. program.

Special appreciation goes to my able mentors Dr. Lawal Garba (Geology), Dr. Sadiq, and all lecturers, Applied Geophysics unit, including, Prof. K.M. Lawal, Dr. A.L. Ahmed, Dr. R. Jimoh, and Mallam. B. Bala, Dr. P. Sule for the educative and quality knowledge of Geophysics they exposed me to.

Further appreciation goes to my course mates, colleagues and friends, Yusuf Ayoola, Ahmed Usman "Smart", Matthew Monday OGWUCHE, Rabiu Ibrahim, , Faruk Raji, Edward Duniya, Kabir Momoh, Ahmed Kundak, Yusuf Siraj, M.B. Sani, Abdulrasheed Adamu, Lawal M. Aliyu, Aminu M. Sani (Al-Ameen), Hammad Ahmad, Larry Bagudu, Mr. Daniel Eshimiakhe, Abu Ubaida Sagir, for the support and solidarity shown me. I wish you all successful undertakings in your future endeavours.

To my Uncle, Dr. Braji Ibrahim and his wife Dr. Zainab Braji (mama), my family inlaws: Captain Rabiu Yadudu, his wives Zainab (Mummy), and Saratu (Anti), Prof. Auwalu Yadudu, Siblings, Alhaji Ibrahim Ibrahim Braji, Rabiu taller, Hamisu, Ahmed, Alhaji Ibrahim Dangudidi, Khamisu Umar (nicknamed BUHARI), Adams, Shehu officer, Musa, Muhd, Bilal, Teema, Nur, Haneefa, Dr. Ummeey Sudan and Friends: Aminu Yusuf Ibrahim (Galadima), Usman feena, Muftahu accountant NCAT Zaria and National Comrade Tijjani Shehu cruch, Sagir Aliyu (Bigshow), Salisu Abubakar Janko, Abdullahi Bature (nicknamed Alhaji Ashiru), Mal. Abubakar, Bello, Baffa Ringim, Salisu Abu Muhd(Dan asabe), Mal Sani mai lemo, Saddam, Don saif, Muhd Babba, Dahuru (Direban amarya), Musa Tullu, Imrana (nicknamed Senior Bachelor), Ilyasu Liman, Sani Sancity, Sunusi Yarima, Fahad, Manager Zoo road, Isyaku (Gyallesu), Adamu Garwa Galan, Yusuf Ringim, Muhd Said Manager (Chairman M.S Global), Abdullahi Lajeen, Abdulmudallib (Hamir Investment), Abba Sleeping, Hamza Comrade, and my Gentle business partner Idris yumbu, and lastly The most senior Gum….Abdul MRS Manager will never forget to acknowledge your unalloyed support I say thank you. God bless you all.

Unreserved appreciation, unexplainable, incomparable, immeasurable, unlimited thanks and prayer, the grand bulldozer, the great exemplary leader and always supportive in any circumstances, the person that never say I can’t, in person of ALHAJI HAMISU RABIU (Chairman Hamir Investment) May Allah (SWT) full fill your wish and make Hamir Investment A World Conglomerate. Ameen.

ABSTRACT

Detailed ground radiometric survey covering 400m x 400m of part of Lere sheet, Kaduna state, Nigeria was carried out. The research was aimed at determining the radiogenic heat production and geothermal potentiality around Rafin Rewa, Dan Alhaji the study area. The number of points used for the data collection were 400 on 20 profiles spaced 20m apart. A map of radioactive heat production was produced and anomalous areas were detected from the map. It was observed that high anomalies were recorded on the western part of the study area with coordinates 8^0 30′ 54″N and $10^0$25′34″E. The results of the study showed a range of radioactive heat production varying from 0.155μWm^{-3} to 154.54 μWm^{-3} with mean value of 31.993 μWm^{-3}. This is higher than the Global mean value of Radioactive Heat Production which is 2.8 μWm^{-3}. This implies that most of the area is suitable for geothermal exploration with the best drilling points on the western part of the area. Comparing the radioactive heat production map with the contour map of individual radioelements maps and ternary image map, this study has shown that Uranium and Thorium are the major contributing elements to the radioactive heat of the study area.

TABLE OF CONTENT

Content **Page**

LIST OF FIGURES AND PLATES

Figures
Page

LIST OF TABLES

Table **Page**

LIST OF ABBREVIATIONS AND SYMBOLS

N	North
E	East
W	West
NE	Northeast
NW	Northwest
SE	Southeast
SW	Southwest
NW-SE	Northwest-Southeast
NE-SW	Northeast-Southwest
W-E	West-East
M	Metre
Km	Kilometre
°	Degree
′	Minute
″	Seconds
et al	and others
e.t.c	and so on
e.g	example
<	Less than
>	Greater than
www	World wide web
K	Potassium
U	Uranium
Rb	Rubidium
Th	Thorium
Cs	Cesium
Be	Beryllium

Nb	Nobium
Pb	Lead
µ	micro
W	Watt
PPM	Part per million
Wt %	Percentage concentration
Bq	Bacqurel

CHAPTER ONE

GENERAL INTRODUCTION

1.1 GENERAL OVERVIEW

Geophysical methods play a great role in exploration of geothermal energy. Exploitation of geothermal resources for energy is common practice in areas where geothermal gradients are high, such as tectonically active regions and in volcanic areas e.g., Iceland and Italy (Yarima *et al*., 2013, *Pasquale* and vedoya, 2000). As demand for sustainable energy increases, and the technology to harness it improves, geothermal resources in relatively quiet regions prove increasingly viable. Geophysical surveys are targeted at measuring the geophysical parameters of the geothermal systems either directly from the surface of the earth or from shallow depth. Recent works by Garba *et al., (2012)* have shown great potential for geothermal heat flow in the Rafin Rewa. Hence, this study has been initiated to gain insight into the geothermal prospect of the study area at Rafin Rewa, Dan-Alhaji village using radiometric method. A geothermal system consists of the following:

i. A heat source,
ii. A reservoir/rock,
iii. A fluid which carries and transfers heat and a recharge area, Yasuka *et al.*, (2005).

By far the biggest source of crustal heat is radioactive isotopic decay which, depending upon geographic location, is estimated to generate up to 98% global heat, (Slagstad,

2008). Other contributions, such as cosmic neutrino interaction with the Earth's mass (Hamza and Beck, 1972) and gravitational distortion (Beardsmore and Cull, 2001), are likely to be very small indeed. The decay of the unstable isotopes of uranium (^{238}U and, to a far lesser extent, ^{235}U), thorium (^{232}Th) and potassium (^{40}K) provide the largest internal source of crustal heat that is geologically significant today (Brown and Mussett 1993). Using the heat production constant values, assumed or measured density (ρ, kg/m^3) and measured ppm concentrations of uranium (C_U) and thorium (C_{Th}), and wt.% concentration of potassium (C_K), the heat production rate (HPR) can be determined thus:

HPR ($\mu W/m^3$) = $10^{-5}\rho$ ($9.52C_U + 2.56C_{Th} + 3.48C_K$) (Rybach, 1988. Saleem, 2011)… (1)

The heat source is due to either radioactivity or active tectonics which represent major zones of magmatic matter that is cooling (Uysal, 2009).

Radiogenic heat values in the crust in conjunction with heat flow density data, contribute to our knowledge of the structure of the Earth's lithosphere (Taylor and Mcleriannan, 1985; Beardsmore and Cull, 2001; Jaupart and Mareschal, 2003) and heat variation plays an important role in crustal processes (Bea and Zinger., 2003; Sanderson *et al.*, 2004). More practically, areas of high heat production are increasingly being identified as possible targets for hot, dry rock geothermal resources (Hasterok and Chapman, 2011). To this end, radiogenic heat values have been calculated from a dataset of 400 points measured.

Geothermal energy is created by the heat of the earth. It generates reliable heat and emits almost no greenhouse gases. It is a reliable source of power that can reduce the need for

imported fuels for power generation. It is also renewable because it is based on practically limitless resources. In addition, geothermal energy has significant environmental advantages because geothermal emissions contain almost non chemical pollutants or waste. This is especially true for geothermal energy representing a promising option for the environmentally sound and secure generation of heat and electricity. They consist mostly of water, which is re- injected underground. The Earth's internal heat is derived from several sources but there are two main sources: (1) the cooling of the Earth since its early history, when internal temperature was much higher than they are now. (2) The heat produced by the decay of long- lived radioactive isotopes. The second is the main source of the earth's internal heat, which in turn, powers all geodynamic processes (Philip, 2005). The Earth is constantly losing heat from its interior, which is many times larger than the energy lost by other means, such as the changes in Earth's rotation and energy released in geothermal flux.

The various geothermal techniques in use for exploration of geothermal energy include subsurface (Shallow) temperature measurement (Lachenbrunch *et al.*, 1997; Kintzinger, 1956; Lee, 1997; LesSchach *et al.*, 1993; Ranmingwong *et al*, 2000); Geochemical thermometric methods (Bandwell , 1965; Magnetolluric methods (Johnson et al, 1992; Gravity method (Johnson, 1995; Sumintadireje *et al*, 2000) Aeromagnetic surveys (Reynold *et al*, 1990; Salem *et al,* 1999, 2000); Seismic Method (Keller, 1981; Rajver *et al*, 1996) and Radioactive Method (Pasquale *et al*, 1997; Louden *et al*, 1996). Each of these methods has its own advantages and disadvantages. Some lack the maturity under difficult conditions while others become less useful for deep exploration because of lack of sensitivity.

Surveying for radiometric minerals has become important over the last few decades because of the demand for nuclear fuels (Keller, 1981; Ehinola *et al.*, 2005). Radiometric surveys are of use in geological mapping as different rock types can be recognized from their distinctive radioactive signature.

In this study, the radiometric method would be used, which involves measuring the concentration of radioactive elements: potassium (K^{40}), Uranium (U^{238}, U^{235}) and Thorium (Th^{232}), using Gamma- ray spectrometer. The gamma-ray method is widely used in Earth Sciences for the determination of naturally occurring radioactive materials. Heat produced by radioactive decay in rocks is of the fundamental importance in understanding the thermal history of the Earth and interpreting the continental heat flux data (Chiozzi *et al*, 2000, 2007).

Geothermal heat exists deep inside the earth's interior and usually appears close to the earth's surface through the means of conduction, convection and Radiation. The heat that emanates from the earth's crust is as a result of the decay of radioactive isotopes of Uranium, Thorium, and Potassium from the earth crust-core which has a temperature of $1000-4500^{0}$C (Nemzer *et al*. 2009).

1.2 Location of the Study Area.

The study area is located in Dan-alhaji, Lere local government, Kaduna State, Nigeria. It is approximately 4 hour, 57 minute drive via Zaria-Panbeguwa-Jos road to Lere to Dan-alhaji (125km) to exact study location (128km). It is flanked at the north by Rishiwa and Geshere Ring Complexes respectively. The study area lies between latitude $10^{o}25'00''$N to $10^{o}25'44''$N, and longitude $8^{o}30'00''$E and $8^{o}30'59''$E. The exact location of the hot spring manifestation is at $10^{o}25'35.7''$N and $8^{o}30'47''$E with an elevation of 729m.

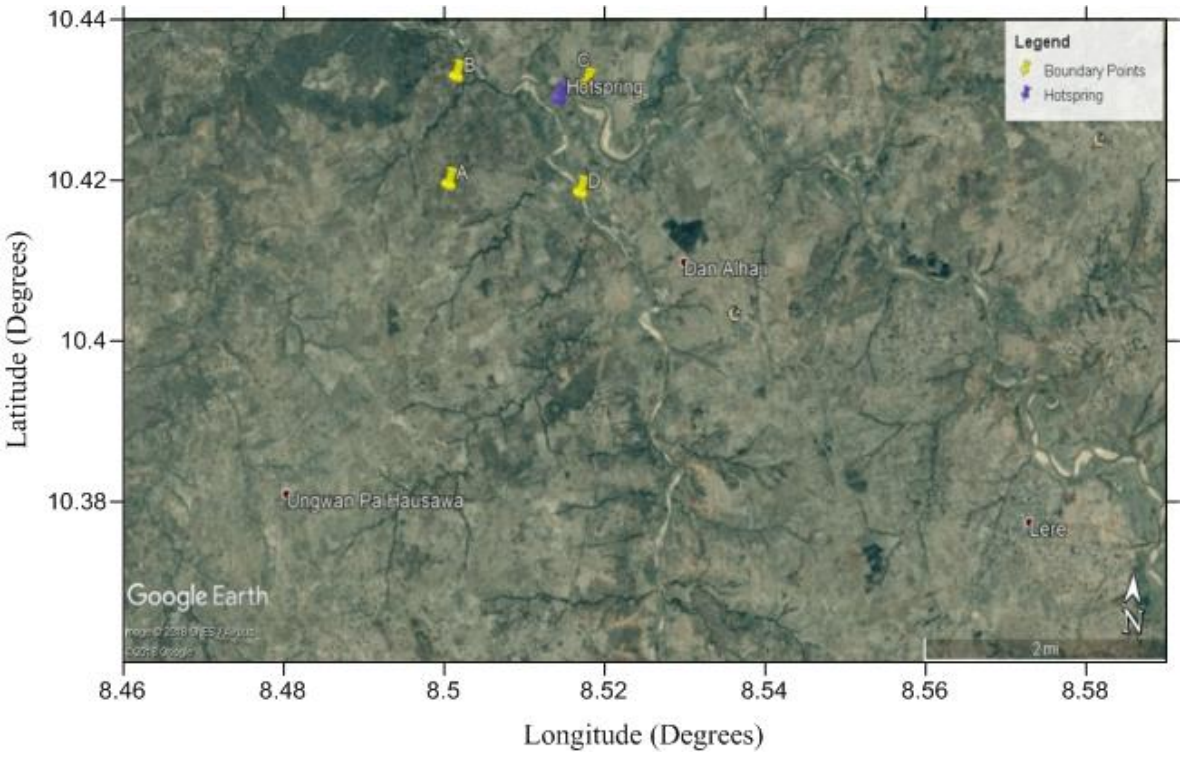

Figure 1.1: Google Earth Map of the Study Area.

Plate 1. The exact hotspot showing Al-Ameen.

1.3 Origin of Rafin Rewa Warm Spring.

Rafin Rewa warm Spring is an ascending perennial spring that yields up to 0.1 l/s, flows from an unconfined aquifer, made up of saprolite, mostly gritty clays and clayey sands derived from the Weathering of migmatite on the Precambrian crystalline rocks of Northern Nigeria (Garba *et al*., 2012). The water is fresh and alkaline, with a mineralization of 318

mg/l. The predominant cation is sodium, with 88.51 mg/l, while the predominant anion, bicarbonate is 207.0 mg/l. A gas with the smell of hydrogen sulphide bubbles and emanates from the spring as its water ascend to the surface. The water and gas are of endogenic origin, flowing from depth not less than 700 metres below ground level, thus making the spring the only known occurrence of juvenile water in Nigeria (Garba *et al*., 2012).

1.4 Geological Setting of the Study Area

The area is located at the fringes of the Jos Plateau, to the SW (fig. 1.2), the centre of the Nigerian Orogenic Younger Granite province of Jurassic age, and directly east of the nearby Rishiwa ring complex. The area is well drained by a good network of rivers most of which take their source from the nearby ring complexes of the Jos plateau (Fig.1.2). The Geology is composed of migmatite gneiss (fig. 1.3) as the oldest rocks, Pan African granites and bauchites (Garba *et al.,* 2012). The bauchite is an unusual rock of acid to intermediate composition, containing, in addition to fayalite, extremely iron rich pyroxenes (ferrohedenbergite and orthoferrosilite), Oyawoye and Makanjuola(1972). The topography of the area is more or less flat laying with the migmatites occurring as low lying exposures, while the granitic rocks stands out conspicuously thereby dotting the landscape.

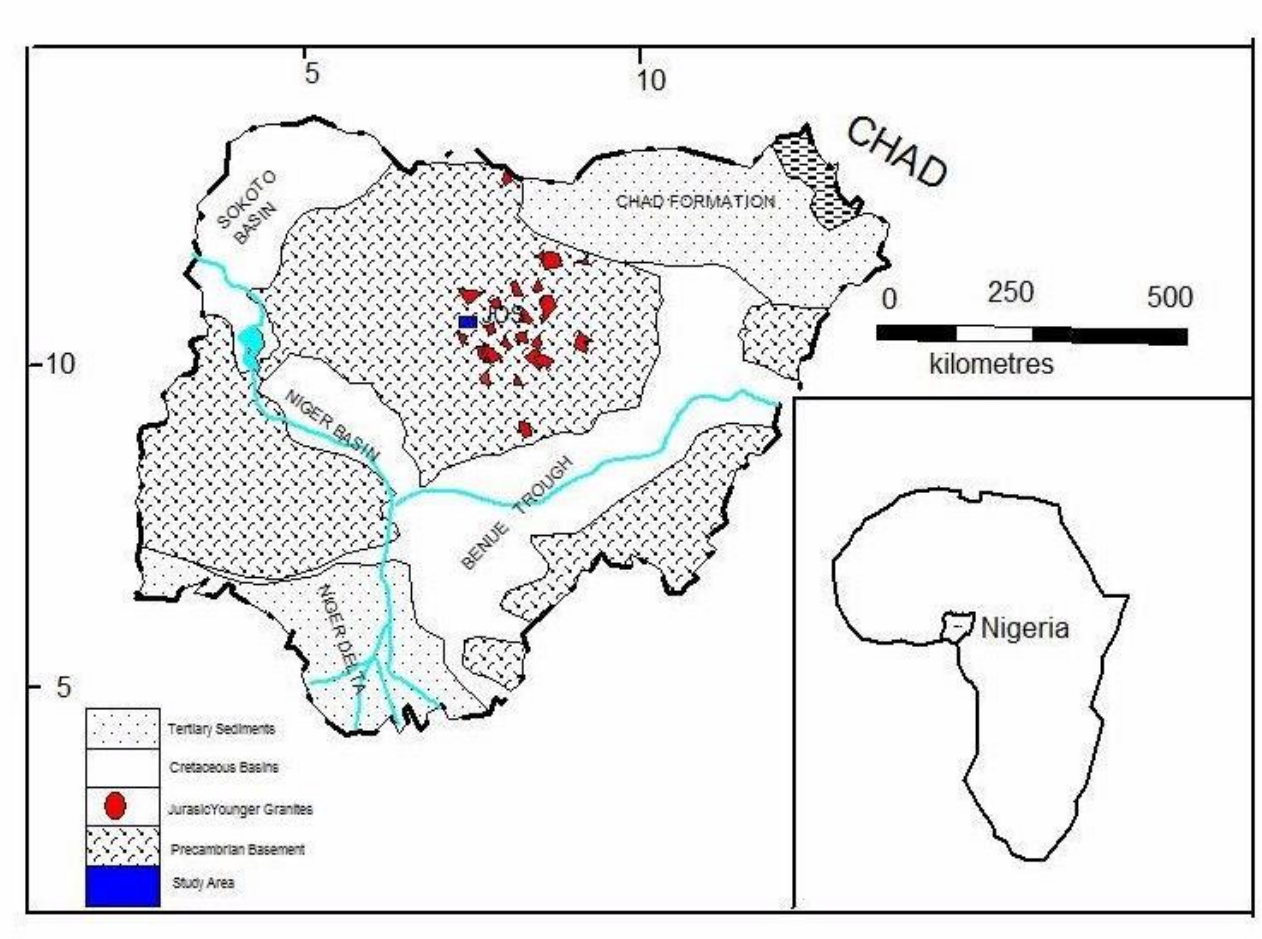

Figure 1.2: Geological Map of Nigeria Showing the Study Area (Garba *et al*., 2012).

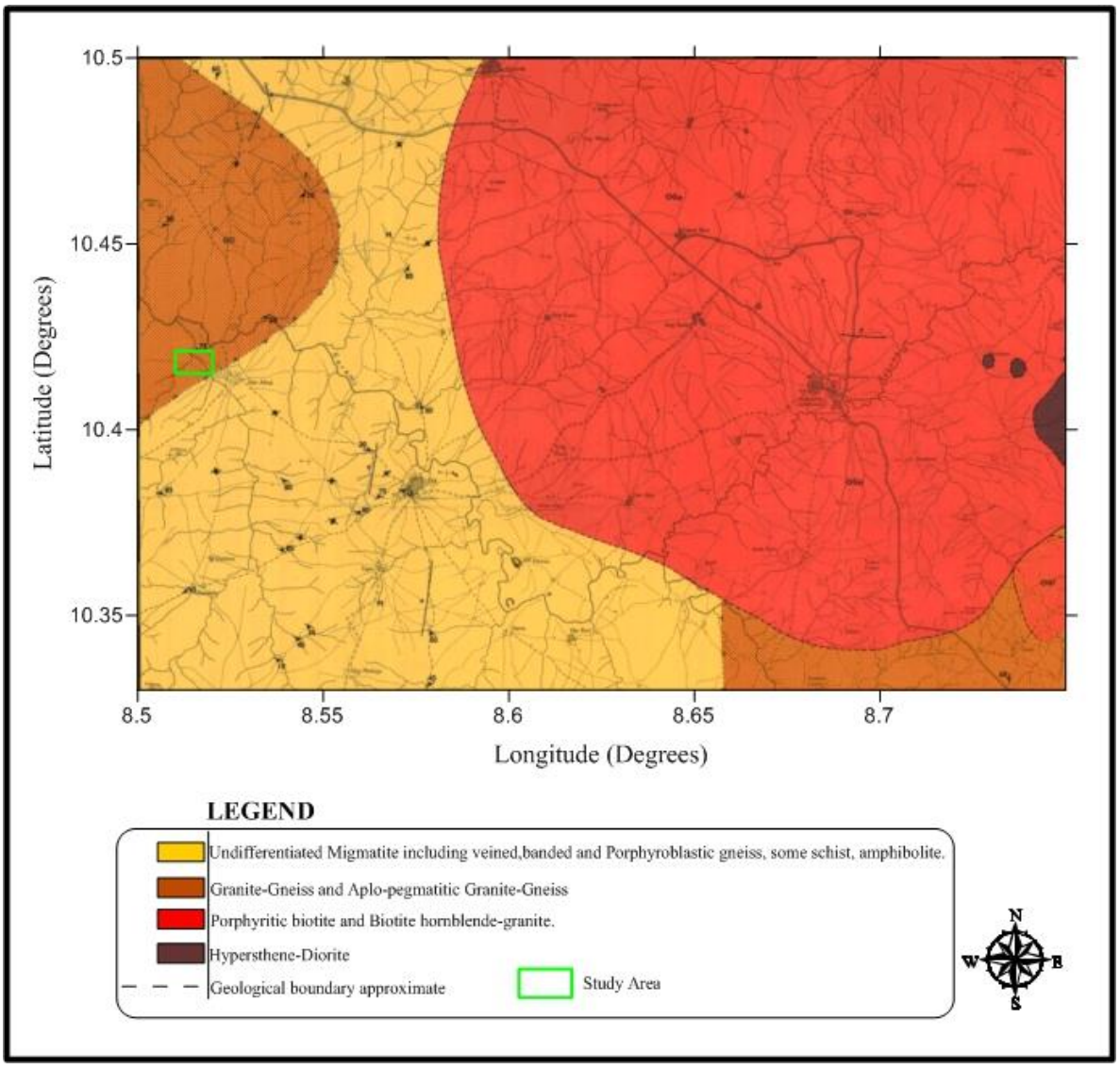

Figure 1.3: Simplified Map of Lere's Bedrock Geology Showing the Approximate Location of the Study Area (adopted from NGSA 1962).

1.5 Statement of the Research Problem

There was a report from Dan-Alhaji village indicating the existence of a spring referred to as "Ruwan Zafi" mostly used by locals for bathing, washing and even spiritual purposes. Although, Nigeria has placed so much emphasis and priority to energy from crude oil and natural gas for generating power and many more, environmental pollution that arises from crude oil exploration processes always remain the main concern. As a result there are calls

for developing environmental friendly energy source (Ewa and Schoenich 2010). And also, based on available literature, no geophysical work has been done to map out the source of heat of the hot spring in the area. As a result of that current research used radiometric method to determine radiogenic heat around Rafin Rewa, dan alhaji village, Lere, Kaduna state, Nigeria. Since existence of hot-spring manifestation in the area is a clear indication of possibility of geothermal resources in the study area.

1.6 Justification of the research.

Geothermal energy is an important source of environmentally friendly and clean energy that has very low environmental hazards that is always associated with using fuel. There is a need to carry out research in every aspect of developing geothermal sources in Nigeria. The manifestation presently in the study area drew the attention of the researcher to conduct the geothermal research there.

1.7 Aim and Objectives.

The main aim of the present study is to carry out a detailed ground spectrometric survey in order to identify possible source of radioactive heat production within the study area for geothermal energy potentials.

The objectives are:

- To determine the concentration of radioactive elements distribution in the study area.
- To determine areas of high radiogenic heat as promising geothermal potential zones of interest.
- Identify the suitable geothermal drilling targets.

CHAPTER TWO

LITERATURE REVIEW

2.1 Historical review of geothermal Energy

Since the nineteenth century, man has become increasingly dependent upon fossil fuels to maintain and improve his standard of living, and the economic ease of obtaining these to date has led to blindness as regards the future. Not so many years ahead, oil and coal, non-renewable resources in human terms, will run out at 2060 (Olumide *et al*., 2015) and in any event, political factors can deprive the use of them at any time (Bowen, 1979). Also, the often deleterious environmental effects of our existing energy sources have been ever more apparent in recent years. Oil spills, strip mining, the emission of Sulphur, Carbon monoxide and accumulation of wastes have emphasized the need for alternative clean energy. One alternative energy may well make a significant contribution and that is geothermal energy. This new source will increase in significance simply because petroleum reserves will probably be depleted within 70 years of exploration (Olumide *et al*., 2015, Bowen, 1979).

Early industrial applications include chemical extraction from the natural manifestations of streams, pools, and mineral deposits in the Lardello region of Italy with boric acid being extracted commercially starting in the early 1800s.

At chaudes-Aigues in the heart of France, the world's first geothermal district heating system was started in the 14^{th} century and still ongoing.

The oldest geothermal district heating project in the United States is on warm springs Avenue in Boise, Idaho, on line in 1892 and continues to provide space-heating for up to 450 homes (world geothermal proceeding 2005).

2.2 Geothermal Energy

Geothermal energy is the energy in form of heat that continually flows outward from deep within Earth. The heat originates primarily in the core. Part of the heat is generated in the crust, the planet's outer layer by the decay of radioactive elements that are in all rocks (Nemzer *et al*., 2009). The crust, which is about 5-75km thick insulate the surface from the hot interior which at the core may reach temperatures from 4000-7000^{o}C (7200-12600^{o}F).

It has been known for many decades that temperature as measured in mines and boreholes increase with depth. This suggests that the Earth's interior is warmer and therefore, the heat must be flowing upward in the Earth (Sharma, 1997). This outflow of heat is almost imperceptible on the earth's surface except at a few localities where heat is somehow dramatically transferred from the Earth's interior through volcanoes and hot springs.

By 1870, modern scientific methods were used to study the thermal regime of the Earth (Bullard, 1965), but it was not until the twentieth century and the discovery of the role played by radiogenic heat, that full comprehension of such phenomena as heat balance and the Earth's thermal history began. All modern thermal models of the Earth, in fact, must take into account the heat continually generated by the decay of the long-lived radioactive isotopes of Uranium(U^{238}, U^{235}), Thorium(Th^{232}) and Potassium(K^{40}) which are present in the Earth (Lubimova, 1968).

Generation of new oceanic crust at spreading centres such as the mid-Atlantic ridge, motion of the lithosphere plates, uplifting of mountain ranges, and release of stored strain energy by the Earthquakes and eruption of volcanoes are all powered by the outward transport of internal heat.

The total flow of heat from the Earth is estimated at 42×10^{12} watts for all of the (convection, conduction and radiation), of this value, 8×10^{12} watts comes from the crust, which represents only 2% of the total volume of the Earth but is rich in radioactive isotopes, 32.3×10^{12} watts comes from the mantle, which represents 82% of the total, and 1.7×10^{12}watts comes from the core, which accounts for 16% of the total volume and contains no radioactive isotopes(Stacey and Lopper, 1988). Worldwide studies of heat flow have provided information on the broad characteristics of thermal conditions beneath the major geological features, including continental rifts, oceanic ridges, subduction margins and intraplate zones of anomalous thermal activity.

Geothermal studies on the region scale have become all the more important because of the energy crisis of the 1970s when it became imperative to consider geothermal energy as one of the several energy sources to displace the use of oil (Sharma, 1997).

2.3 Hot Springs

Hot spring also called thermal spring, is spring with water at temperatures substantially higher than the air temperature of the surrounding region (encyclopaedia Britannica).

The water issuing from a hot spring is heated by geothermal heat i.e. heat from the earth's interior. In general, the temperature of the rocks within the earth's increases with depth.

The rate of temperature increase with depth is known as the geothermal gradient. If water percolates deeply into the crust, it will be heated as it comes into contact with hot rocks. As it descends through the rock, it picks up a variety of materials, everything from radium to Sulphur. Also, as it moves further the primal heat of the earth, it eventually encounters a large thrust fault, or cracks. As water descends behind it, it forces the now heated water to ascend along the fault line to surface as hot or warm spring. The water from hot springs in non-volcanic areas is heated in this manner. In active volcanic zones, water may be heated

by coming into contact with magma (molten rock). The high temperature gradient near magma may course water to be heated enough that it boils or becomes super-heated, if the water becomes so hot, erupt in a jet above the surface of the Earth, it is called a geyser. If the water only reaches the surface in the form of steam, it is called a fumarole. If the water is mixed with mud and clay, it is called a mud pot (Encyclopaedia Britannica 2018).

2.4 Radiogenic Elements and Heat Production.

Radiogenic Elements: Uranium, Thorium and Potassium

Energy released by short- lived radioactive isotopes may have contributed to the initial heating, but the short- lived isotopes would be consumed quite early. The heat generated by long- lived isotopes has been an important heat source during most of Earth's history. In order to be a significant source of heat, radioactive isotopes must have a half- life comparable to the age of the Earth, the energy of its decay must be fully converted to heat and isotopes must be sufficiently abundant. The main isotope ^{235}U has a shorter half- life than ^{238}U and release more energy in its decay.

2.5 Heat Transport and its Distribution within the Earth

Numerous attempts have been made to interpret Earth's dynamic processes based upon heat transport concepts derived from ordinary experience. But, ordinary experience can be misleading especially when underlain by false assumptions. Geodynamic considerations traditionally have embraced three modes of heat transport: conduction, convection and radiation.

Recently, investigation shows that, there may be fourth; "mantle decompression thermal tsunami" (Marvin, 2010), and speculate that there might be a fifth mode: "heat channelling", involving heat transport from the core to "hot-spot" (Marvin, 2010) such as those that power the Hawaiian Islands and Iceland.

2.5.1 Heat Convection: Convection is heat transfer by means of mass motion of a fluid such as air or water when the heated fluid is caused to move away from the source of heat, carrying energy with it. **Convection** above a hot surface occurs because hot air expands, becomes less dense, and rises. (Encyclopaedia) Or **Convection** is the transfer of energy by movement of a medium, whereas **radiation** is the transfer of energy by, well, thermal **radiation**. **Conduction** also requires a medium, but, again, it is a fundamentally different mechanism than either **convection** or **radiation**; in this case it is the transfer of energy through a medium. (Encyclopaedia 2010)

2.5.2 **Conduction** is the process by which heat energy is transmitted through collisions between neighbouring molecules. (Encyclopaedia Britannica 2018)

2.5.3 **Radiation** is the transfer of heat energy without the involvement of a physical substance in the transmission. Radiation can transmit heat through a vacuum. Energy travels from the sun to the Earth by means of electromagnetic waves. The shorter the wavelength, the higher the energy associated with it.

The absorption of radiant energy by matter increases its temperature and there by the temperature gradient.

2.6 Earth Internal Heat Sources.

About one-third of the heat flow comes from the original heat in the Earth's core and mantle (the layer closest to the Earth's crust) (Physics of the solid earth 2015). The remaining two-thirds originate from radioactivity in the Earth's crust, where radioactive substances continuously decay and generate heat. Heat from radioactive-decay of ^{235}U, ^{238}U, ^{232}Th, and ^{40}K has long been considered as the main energy source for geodynamics processes, geomagnetic field generation, and for the Earth's heat loss (Pollack *et al*, 1993). For more

than half a century, geophysicists have made measurements of near-surface continental and oceanic heat flow with the aim of determining the Earth's heat loss.

Confusion as to the nature of location and nature of radionuclide energy sources within the Earth stems from the mistaken belief, prevalent for the past hundred years, that the Earth is like an ordinary chondrite meteorite rather than, as it was discovered thirty years ago, a highly-reduced enstatite chondrite(Herndon,1979,1980,1982,1998 and 2005).

In ordinary chondrites, which formed under more oxidizing conditions than enstatite chondrites (Herndon, 2007), all of the radionuclides are found in the silicate portion. It has been assumed that, these would occur exclusively in the Earth's mantle and crust. Reports, however, have suggested that at high pressures 40K might occur in the Earth's core (Murthy, *et al*, 2003). The absence of core-heat sources in an "ordinary-chondritic Earth" led to the *ad hoc* suggestion, without corroborating evidence, that the inner core is growing by freezing, releasing the heat of crystallization which hypothetically provides useful energy rather than just slowing the assumed rate of freezing.

The identification of the endow-Earth (lower mantle plus core) with an enstatite chondrite(Herndon,2005) made it possible to deduce that the bulk of Earth's uranium resides within the core and to demonstrate the feasibility of its functioning as a natural nuclear fission reactor (Herndon,1993,1994,1996 and 2003, Hollenbeck, *et al*, 2001). The nuclear georeactor is an unanticipated deep-Earth energy source that produces the Earth's magnetic field (Herndon, 1993, 1994, 1996, 2003 and 2009, Hollenbeck, *et al*, 2001). Energy production from the nuclear fission of Uranium is significantly greater than from its radioactive decay, but may consume Uranium at a much greater rate. It is an open question as to whether thorium, possibly also in the Earth's core, exists under circumstances that

might permit it to be converted to fissionable ^{234}U and thereby produce more energy than by radioactive decay alone.

The identification of the endo-Earth with an enstatite chondrite made it possible to deduce from thermodynamic considerations the circumstances of Earth's early formation as a Jupiter-like gas-giant and to reveal another major, unanticipated energy source, the stored heat of protoplanetary compression (Herndon, 2006). This vast energy source is responsible for fracturing Earth's 100% closed, contiguous, continental-rock shell, for decompressing Earth and for powering Earth's compression-driven geology, as described by whole-Earth decompression dynamics (Herndon, 2005 and 2010), and for emplacing heat at the base of the crust (Herndon,2006).

2.7 Geothermal Resources.

Exploitable geothermal resources originate from transport of heat to the surface through several geologic and hydrological processes. Geothermal resources commonly have three components:

(1) A heat source, (2) high relatively permeability reservoir rock, and (3) Fluid to transfer the heat.

In general, the heat source for most of the high temperature (>150^{o}C) appears to be a molten or recently solidified intrusion, where as many of the low temperature (<100^{o}C) and moderate temperature resources (between 100^{o}C and 150^{o}C) seems to result from deep circulation of meteoric water with heating due to the normal increase in temperature with depth. The classification of geothermal resources is shown in Table 1.1 below. The table summarise the way that geothermal resources are commonly classified. For the most part, only convective hydrothermal resources have been commercially developed. The other

resource types will require new technology and /or higher energy prices in order to be more economical.

Geothermal energy was explored for generating electrical power in 1904 in Tuscany, Italy. Geothermal are also used to heat buildings in Budapest, Hungary, a Paris suburb, Iceland, (since 1890) part of Boise, Idaho (World geothermal proceeding 2015).

At the beginning of the 21st century, there were some 380 geothermal power plants in 22 countries around the world with a combined installed capacity of about 8000 megawatts. But in current report from international geothermal association (IGA), and Annual U.S and global geothermal power production report 2016 that there were about 12,640 geothermal plants operating around the globe. The present value of world energy tapping from geothermal stopped at 12.6 GW confirming from trend started in 2020 (annual global geothermal power production, 2016).

Henceforth, if geothermal project will continue till 2050 then average of 140 GW will be reached and if the target of 140 GW could be reached, it would be possible to produce from geothermal up 8.3% of total world electricity production, serving 17% of world population. Moreover, 40 countries (located mostly in Africa, Central/South America, Pacific) can be 100% geothermal powered. The overall CO_2 saving from geothermal electricity can be in around 1,000 million tons per year. The electricity produced from geothermal power in the United State represent about 37 percent of the world's output of electricity from geothermal power. The united states, Philippines, Italy, Mexico, Indonesia, japan, new Zealand, Egypt, turkey, Germany, Costa Rica, Mexico and Iceland are the largest producers of geothermal energy (Nember *et al.,* 2009).

In Nigeria the Ikogosi spring is located within quartzite-schist formation of Nigerian basement complex. The temperature of the spring water is 37°C. It is used as swimming

pool being a significant local tourist attraction and probably the only place of geothermal (direct) use in Ekiti state, Nigeria. The Wikki warm spring having a temperature of 32^{o}C flowing from Gombe Sandstone in Yankari Game Reserve in Bauchi state, North eastern Nigeria are the two main known geothermal resource areas in Nigeria (Garba *et al*., 2012).

There is another warm spring recently discovered in Rafin Rewa, Ruwan zafi spring in dan-Alhaji village,near Lere Kaduna state, to the north-west of Jos Plateau (central shield). The temperature of spring water is 42°C (study area) and it flows from magmatic and gneissic rock formation (Garba *et al*., 2012). Several springs have been known to exist in Jos Plateau and all of them provide cold, fresh water, commonly used by local community. The existence of Ikogosi warm spring and that recent discovery suggest that distribution of geothermal heat within Precambrian basement formations in Nigeria can be diversified due to local anomaly. Another hot one (54°C) is located in the North of Benue Trough, within a huge tectonic structure -Lamurde anticline, nearby Numan and is called Ruwan Zafi. The water of the springs is heated by geothermal gradient on its way from unknown depths, in unconfined sandstone aquifer (Garba *et al*., 2012).

Within the Middle Benue Trough several minor thermal seepages were found nearby Awe where the temperature of the water ranges from 34 to 38.5°C. Warm water is provided to the surface also by two artesian wells found in that area. Temperatures of the water flowing from those wells are 43.5°C and 34°C. They were drilled in the end of 1970s or beginning of 1980s and left for the local community as a source of domestic water. Today the water is still freely flowing there but the depth of the wells as well as features of the aquifer are unknown and drilling documentation obviously does not exist. (Garba *et al*., 2012).

Table 1.1 Geothermal Resources Classification after Wright (1998)

Geothermal Resources Classification	
Resources Type	Temperature characteristics
Convective Hydrothermal Resources:	
Vapour dominated	240˚
Hot-water dominated	20 to 350˚+
Other hydrothermal resources:	
Sedimentary basin	20 to 150˚
Geopressured	90 to 200˚
Radiogenic	30 to 150˚
Hot rock resources	
Solidified (hot dry rock)	90 to 650˚
Part still molten (magma)	>600˚

Based on Donald's (1957) Classification, it can be concluded that the water of Rafin Rewa warm spring may have originated from the Quaternary to Recent magmatic activity that affected the Jos Plateau area of Nigeria, and which possibly after mixing with meteoric water flows out as an ascending spring through regional lineaments that transcends the area. These lineaments which have a regional extent have also been mapped by previous worker (Garba *et al.,* 2012).

2.8 Principle of Radioactivity.

The application of radioactivity in geoscience is based on knowledge of the physical properties of radiation sources, and our ability to detect these sources through the analysis of spectrometric data. This chapter reviews the principles of radioactivity and its detection

2.9 Bases of Radioactivity.

Radioactivity is the process where an unstable atom becomes stable through the process of decay, or breakdown of its nucleus. During decay, energy is released in the form of three types of radiation: alpha (α), beta (β) particles and gamma (γ) radiation. This process is called: Radioactive decay.

Atoms are the smallest particles of mass with distinctive chemical properties. An atom consists of a nucleus surrounded by electrons. The nucleus consists of positively charged protons, and uncharged neutrons. The diameter of an atom is of the order 10^{-10} m, and the diameter of a nucleus is of the order 10^{-15} m. Protons and neutrons have a mass of 1.67×10^{-27} kg. The mass of negatively charged electrons is 9.11×10^{-31} kg. The elementary charge is 1.602×10^{-19} C.

The number of protons in a nucleus of an element, X, is the proton number Z (also called the atomic number). The sum of the protons and neutrons (nucleons) is the mass number, A, of an atom. Atoms of an element having the same atomic number but different numbers of neutrons (i.e. different mass numbers) are called *isotopes*. Isotopes are denoted by their chemical symbol and their mass number as follows - AX. Isotopes have identical chemical properties, but different physical properties. Atoms having identical numbers of protons and neutrons are named nuclides.

The atomic nuclei of some isotopes have a surplus of energy, are unstable, and disintegrate to form more stable nuclei of a different isotope. This process is accompanied by the emission of particles or energy, termed nuclear radiation. Nuclides with this feature are called radionuclides, and the process is called nuclear decay or disintegration.

The radioactivity decay law expresses the decrease in the number of atoms of a radionuclide with time:

$$N_t = N_o e^{-\lambda t} \quad \text{(2.1)}$$

Where N_t = the number of atoms present after time t (s);

N_o = the number of atoms present after time $t = 0$;

λ = the decay constant of a radionuclide (s^{-1}),

A related constant, the half-life $T_{½}$ (s), is the time taken for half the radionuclides to decay:

$$T_{½} = \frac{0.693}{\lambda} \quad \text{(2.2)}$$

The product gives the activity (Bq) of the radionuclide. Radioactive decay is independent of other physical conditions (IAEA 2003).

2.10 Types of radioactive decay

The type of decay of unstable nuclides determines the nature of the newly formed atoms. The equations representing transitions of an element X to an element Y by a specific mode of decay are summarized as follows:

$$^{A}X \rightarrow {}^{A-4}Y + \alpha \text{ (alpha emission)}, \qquad Z_Y = Z_X - 2 \quad \text{(2.3)}$$

$$^{A}X \rightarrow {}^{A}Y + \beta \text{ (beta emission)}, \qquad Z_Y = Z_X + 1 \quad \text{(2.4)}$$

$$^{A}X \rightarrow {}^{A}Y + \text{photon (electron capture)}, \qquad Z_Y = Z_X - 1 \quad \text{(2.5)}$$

Some radionuclides may have more than one mode of decay. For example, 66 percent of ^{212}Bi disintegrations are by beta particle emission to ^{212}Po, and 34 percent are by alpha particle emission to ^{208}Tl. But irrespective of the type of radiation, the observed half-life is always the same (Ahmad 2006).

Radioactive decay also often occurs in series (or chain) with a number of daughter products, which are also radioactive, and terminates in a stable isotope. In a closed system, and starting with a specified amount of a mother element, the number of atoms of daughter

elements and their activity grows gradually until radioactive equilibrium of the disintegration series is reached. At this point, the activities of all the radionuclides of the series are identical. Thus the measurement of the concentration of any daughter element can be used to estimate the concentration of any other element in the decay series. Under equilibrium conditions, this relationship can be expressed as follows:

$$\lambda_1 N_1 = \lambda_2 N_2 = \lambda_3 N_3 = \ldots\ldots\ldots\ldots + \lambda_i N_i \qquad (2.6)$$

Examples of chain disintegration are the natural decay series ^{238}U, ^{235}U and ^{232}Th.

2.11 Natural Sources of Radiation

While many naturally occurring elements have radioactive isotopes, only Potassium, Uranium and Thorium decay series, have radioisotopes that produce gamma rays of sufficient energy and intensity to be measured by gamma ray spectrometry.

This is because they are relatively abundant in the natural environment. Average crustal abundances of these elements quoted in the literature are in the range 2-2.5% K, 2-3 ppm U and 8-12 ppm Th.

^{40}K is the radioactive isotope of potassium, and occurs as 0.012 percent of natural potassium.

This isotope decays to ^{40}Ar with the emission of gamma rays with energy 1.46 MeV. Since ^{40}K occurs as a fixed proportion of K in the natural environment, these gamma rays can be used to estimate the total amount of K present. The half-life of ^{40}K is 1.3×10^9 years (IAEA 2003).

Uranium occurs naturally as the radioisotopes ^{238}U and ^{235}U which give rise to decay series that terminate in the stable isotopes ^{206}Pb and ^{207}Pb respectively (Tables 2.1 and 2.2). The half-lives of ^{238}U and ^{235}U are 4.46×10^9 and 7.13×10^8 years, respectively. Thorium

occurs naturally as the radioisotope ^{232}Th which gives rise to a decay series that terminates in the stable isotope ^{208}Pb (Table 2.3). The half-life of ^{232}Th is 1.39 x 10^{10} years. Neither ^{238}U, nor ^{232}Th emit gamma rays, and gamma ray emissions from their radioactive daughter products are used to estimate their concentrations (IAEA 2003).

2.12 Decay Chain of Potassium, Uranium and Thorium

Natural radioactivity is confined principally to the disintegration of three naturally occurring elements namely; Potassium (K), Uranium (U), and Thorium (Th). In addition to these, there are other naturally occurring radioactive isotopes such as Rubidium (Rb) and the rare earth elements Samarium (Sm) and Lutecium (Lu).

Whereas Potassium undergoes a simple form of radioactive decay the decay of Uranium and Thorium is complex and proceeds sequentially along a chain of disintegration (Ahmad 2006). Each of the particles emitted during radioactive decay has its own characteristics and the gamma rays are characteristics of the elements, which emit them. Natural sources of gamma radiation in rocks originate from the decay of radioactive products in the Uranium and Thorium decay chains and decay of Potassium. The decay chains of U^{238}, U^{235}, Th^{232} and some of the gamma rays emitted by their daughters are shown in tables (2.1) (2.2) and (2.3) respectively.

Table 2.2: The U-238 Series decay chain (Omitting Branching Decays Contributing less than 0.2%) (After Evans 1955)

Name of Isotope	Nuclide	Particle emitted	Particle energy(MeV)	Half life	Energy of gamma rays emitted (MeV)
URANIUM	*GROUP*				
U-1	U^{238}	Alpha	4.20	$4.507x10^{9}Y$	0.047
UX_1	Th^{234}	Beta	0.19	24.1d	0.0093, 0.766, 1.001
UX_2	Pa^{234}	Beta	2.29	1.18	0.394, 0.782
UX		Beta			0.806, 0.820
UII	2-234	Alpha	4.77	$2.48x10^{5}Y$	0.06, 0.093, 0.0118
IONIUM	Th^{230}	Alpha	4.68	$7.52x10^{4}Y$	0.068,0.14,0.190,0.228,0.240
RADIUM	GROUP				
Radium	Ra^{226}	Alpha	4.78	1600 Y	0.188
Radon	Rn^{222}	Alpha	5.49	3.825d	
Ra-A	Po^{218}	Alpha	6.00	3.05m	
Ra-B	Pb^{214}	Beta	1.03	26.8m	0.053,0.242,0.259,0.295,0.351
Ra-C	Bi214	Beta	3.26	19.7m	0.063,0.191,0.426,0.498,0.609,0.766,0.933 2.42,1.12,1.238,1.379,1.52,1.765,1.82,2.204
Ra-c	Po^{214}	Alpha	7.68	$1.5x10^{-4}s$	
Ra-D	Pb^{210}	Beta	0.061	22.3Y	0.007,0.023,0.32,0.37,0.043,0.043,0.047,0.065
Ra-E	Bi^{210}	Beta	1.16	5.02d	
Ra-F	Po^{210}	Alpha	5.30	138.4d	0.084,0.790
Ra-G	Pb^{206}	Stable	-	-	--------

2.3: TABLE DECAY CHAINS OF U-235 (AFTER Evans 1955)

Isotopes	Half life	Particles emitted	Particle energy(MeV)	Gamma-ray Energies (MeV)
U^{235}	$7x10^{8}$Y	Alpha	4.18-4.56	0.095
Th^{231} (U Y)	25.6 h	Beta	0.30	0.084
Pa^{231}	$3.4x10^{4}$ Y	Alpha	4.66-5.046	0.020, 0.39
Ac^{227}	22 Y	Alpha	4.94	-
Tu^{227}	18.2 d	Alpa	5.708	0.24
(Ra-Ac)				
Fr^{223}	22 m	Beta	1.5	0.21, 0.31
(Ac K)				
Ba^{223}	22 d	Alpha	5.712	0.58
Rn^{219}	3.9 s	Alpha	6.547	0.40
Po^{215}	$1.8x10^{-3}$ s	Alpha	7.360	-
At^{215}	$1x10^{-4}$ s	Alpha	8.00	-
Pb^{211}	36 m	Beta	0.5	0.40,0.43,0.80
Bi^{211}	2.16 m	Alpha	6.617	0.35
(Ac-C)				
Po^{211}	0.52 s	Alpha	6.57	0.57,0.89
(Ac-C')				
Tl^{207}	4.79 m	Beta	1.44	-
(Ac-C")				
Pb^{207}	Stable	=	-	-
(Ac-D)				

Table 2.4: The Th-232 Series Decay Chain (After Evans 1955)

Name of isotopes	Nuclide	Particle emitted	Particle energy (MeV)	Half life	Energy of gamma ray emitted (MeV)
Thorium	Th^{232}	Alpha	4.01	$1.4x10^{10}Y$	0.055,0.075
M5Th 1	Ra^{228}	Beta	0.053	6.7 Y	0.030
M5Th 2	Ac^{228}	Beta	2.11	6.13 h	0.060,0.135,0.184,0.33,0.462,0.533,0.590,0.913,0.969
Radiothorium	Th^{228}	Alpha	5.43	1.91Y	0.087
Th-x	Ra^{224}	Alpha	5.68	3.64 d	0.241
Thoron	Rn^{220}	Alpha	6.29	55.3 s	-
Th-A	Po^{216}	Alpha	6.78	0.158 s	-
Th-B	Pb^{212}	Beta	0.58	1.064 h	0.115,0.176,0.238,0.249,0.299
Th-C	Bi^{212}	Beta	2.25		0.4,0.144,0.164,0.288,0.328,0.432,0.452,0.472,0.720
				60.5 m	0.830,1.03,1.34,1.61,1.81,2.20
		Alpha	6.09		-
		(36%)	-		-
Th-C’	Po^{212}	Alpha	8.78	$3.0x10^{-7}$	- -
Th-C”	Tl^{208}	Beta	1.80	3.1 m	0.277,0.510,0.582
64%					0.859,2.62
Th-D	Pb^{208}	Stable	-		-

2.13 Geochemistry of Radioelements.

Potassium

Potassium (K) is an alkali earth metal. Potassium forms a major component in many rock type. Most of these rocks are composed of the silicate minerals such as alkali feldspar, leucite, biotite, muscovite, phlogopite and some amphiboles.

Most igneous rocks have potassium being the main aggregate. The amount of potassium is used for the petrograhic groupings. During magmatic differentiation, potassium is gradually concentrated thus more potassium is concentrated in felsic than mafic igneous rocks. This is observed in the variations in K concentration of basalt, normally less than 1%, and granite, which is composed 2% to less than 6% (Elawadi et al., 2004, Fertl, 1983; Wedepohl, 1978). Dickson and Scott (1997) indicated that during weathering process, the main potassium sources will be destroyed in the order biotite-K-feldspar-muscovite. When weathering is taking place, the freed potassium can be used for the formation of potassium enriched clay minerals like illite or may be taken up in small quantities by other clays (montmorillonite) under better conditions.

The magmatic and metamorphic rocks series control almost all the potassium enriched minerals such as the feldspar mainly the feldspathoids leucite and nepheline, and the micas, biotite and muscovite.

2.15 Thorium

Thorium (Th) is a part of the actinide group of elements. +4 is the main oxidation state of this element and thorium-232 (^{232}Th) as the only natural occurring isotope. Thorium has an incredibly long half-life of 1.4×10^{10} years (Wedepohl, 1978). It is strongly lithophilic and is more abundant within the crust of the Earth. During the decay series of thorium, the parent thorium nuclide disintegrates with emission of gamma radiations of energy 2.62

MeV and ^{208}Tl as the daughter nuclide. Granitic rocks records higher concentration of thorium than mafic igneous rocks. The concentration of thorium normally cannot move but due to environmental conditions there can be a small movement. Thorium fundamentally cannot dissolve in both surface and groundwaters. Therefore it is a helpful guide element in sediments of stream for finding deposits of uranium related with magmatic rocks (Chopin, 1988; Elawadi *et al*., 2004; Krishnaswami, 1999). Monazite and zircon are the main minerals enriched with thorium.

Uranium

Uranium (U) is an extremely heavy element that can be considered as the most radioactive element in the world. Uranium produces the most abundant supply of concentrated energy. Uranium is contained in most soil in amount of 2 to 4 parts per million and is widespread in the crust of Earth. In the crust of the Earth, most of the uranium is a combination mostly of two isotopes ^{238}U and ^{235}U.

Uraninite is widespread as tiny traces in the minerals forming up the rock in granites or as grains in mineralized pegmatites and granites. In addition Uraninite is present in hydrothermal layers and sedimentary rocks. Zircon, Monazite, apatite, Allanite and Sphene (accessory minerals) which are related with igneous and metamorphic rocks are the most resistant to weathering (Langmuir and Hermans, 1980; IAEA, 2003). Uranium released during weathering possibly will be preserved in authigenic oxides of iron and minerals under reducing environment forming deposits of Uranium under conducive conditions (Dickson and Scott, 1997). Uranium itself does not emit gamma-rays during its decay but

the most energetic gamma-rays emitted by its daughter isotopes come from ^{214} Bi which occurs late in the decay series (Dickson and Scott, 1997).

2.14 Distribution of the Radioelements in Rocks and Soils.

For normal rocks and soils, 90% of the gamma rays measured by a spectrometric survey emanate from the uppermost 30 cm to 40 cm of the Earth. The content of potassium in rocks can have a range of 0 to 10% potassium but is usually 1 to 5% potassium with average of about 2% potassium. The content of Uranium and Thorium in rocks changes from near zero to several hundreds of part per million (ppm). The amount of K, U and Th depends on rock type and the geological environment. In most areas beneath the Earth, the bedrock is covered with soil. Hence, the radiation from the soil is the most essential contributor to the terrestrial radiation. The amount of the radiation from minerals in the soil depends upon the content in the original parent rocks (IAEA, 1990). Moreover Potassium is extremely unable to coexist during crystallization of magma. A rock of composition of 2.5% K, 3ppm U and 15 ppm Th could be a granite, felsic intrusive or shale (Dickson and Scott, 1997).

Available data for metamorphic rocks which include gneissic resulting from granite or amphibolites resulting from dolerite suggest that metamorphism does not affect radioelement content. Sedimentary rocks generally have radioelement content reflecting the parent rock source. Hence, young sediments derived from granitic sources may be expected to have quite high radioelement content, but more mature sediments, composed primarily of quartz should have very low values when specific rock types such as pegmatite, aplites, quartzfeldsparporphyrites and mafic intrusives occur as narrow intrusions or in small areas,

or are subjected to faster weathering and erosion than the host country rock, it is difficult to find insitu soils (Dickson and Scott, 1997).

Granite depicts a broad array of weathering behaviour, depending on its mineralogy and the weathering system, climate etc. Soils derived from granitoids generally lose around 20% of their radioelements contents during pedogenesis. Soils over radioelement-poor arenite, as over other poor radioelement-poor rocks; can show the effects of contamination by transported materials (Darnley, 1996).

Processes other than in-situ weathering can affect the radioelement content of soils. They include clay eluviation, colluvial and aeolian transport, and soil movement. All can affect the concentration of radioelements in the thin 30 cm to 40 cm layer measured during aerial surveying (Wilford *et al*., 1997).

2.15 Interaction of Gamma Rays with Matter.

Radiation is comprised of a flux of elementary particles and energy quanta, and can be classified by its physical character and energy. These determine how the radiation interacts with matter.

Alpha radiation is a flux of positively charged alpha particles. Alpha particles have an initial energy of several MeV, and an initial velocity of the order 10^7 m/s. They exhibit high ionization, and their penetration range in matter is low. Alpha particles are absorbed by about 10^{-2} m of air, and 10^{-5} m of rock. Alpha particles have a discrete energy that is specific for a particular radionuclide.

Beta radiation is a flux of electrons with a continuous energy spectrum up to a maximum energy, which depends on the particular radionuclide. The initial velocity of beta particles can approach the velocity of light. The penetration range for beta particles depends on the

initial energy of the particle. For E=2 MeV, the penetration range is about 8 m in air and 1 cm in water.

Beta radiation passing through matter loses its energy by ionization and generates electromagnetic radiation called bremsstrahlung. Positrons passing through matter combine with electrons, and generate two annihilation gamma quanta of energy 511 KeV each.

Gamma radiation is part of the electromagnetic spectrum. Gamma rays travel at the speed of light (c), and have a discreet energy (E), frequency (f), and wave length (λ). These are related by:

$$E = hf = hc/\lambda \qquad (2.7)$$

Where h = Planck's constant 6.6261×10^{-34} Js;

c = velocity of light.

Electromagnetic radiation of energy E <40 keV is denoted as X-rays. Gamma rays comprise that part of the electromagnetic spectrum where E >40 keV.

Gamma rays interact with atoms of matter by three principal processes (ICRU, 1994). These are the photoelectric effect, Compton scattering and pair production. The photoelectric effect is the predominant absorption process at low energies, and results in all the energy of a gamma quantum being absorbed in a collision with an electron of an atom. Compton scattering predominates at moderate energies and corresponds to a collision of an incident photon with an electron. The incident photon loses part of its energy to the electron and is "scattered" at an angle to its original direction. Pair production occurs at energies greater than 1.02 MeV. It is the process whereby an incident photon is completely absorbed and results in the creation of an electron-positron pair in the electrostatic field of a nucleus (IAEA, 2003).

Typically, gamma ray photons lose energy through successive Compton scattering events, until eventually the resulting low-energy photons are absorbed through the photoelectric effect. As a result of the interaction of gamma rays with matter, the intensity of radiation decreases with distance from the source. The absorption of gamma rays of a specific energy in matter is described by either a linear attenuation coefficients μ (m^{-1}) or a mass attenuation coefficient μ/ρ (m^2/kg). For a narrow beam of gamma rays, the attenuation of the gamma rays can be modelled by an exponential function. The range of gamma rays of natural radionuclides is about 700 m in air, up to 0.5 m in rocks and a few cm in lead. Gamma rays have a discrete energy that is specific for a particular radionuclide. Since gamma rays are the most penetrating component of natural and man-made radiation, they are widely used in the study of the radiation environment (IAEA, 2003).

2.16 Disequilibrium

Disequilibrium occurs when one or more decay products in a decay series are completely or partially removed or added to the system. Thorium rarely occurs out of equilibrium in nature, and there are no disequilibrium problems with potassium. However, in the uranium decay series disequilibrium is common, and can occur at several positions in the ^{238}U decay series: ^{238}U can be selectively leached relative to ^{234}U; ^{234}U can be selectively leached relative to ^{238}U; ^{230}Th and ^{226}Ra can be selectively removed from the decay chain; and finally ^{222}Rn (radon gas) is mobile and can escape from soils and rocks into the atmosphere. Depending on the half-lives of the radioisotopes involved, it may take days, weeks or even millions of years for equilibrium to be restored.

Disequilibrium in the Uranium decay series is a serious source of error in gamma ray spectrometry. Uranium concentration estimates are based on the measurement of ^{214}Bi and ^{214}Pb isotope abundances. These occur far down in the radioactive decay chain and may not be in equilibrium with Uranium. Estimates of Uranium concentration are therefore usually reported as "equivalent Uranium" (eU) as these estimates are based on the assumption of equilibrium conditions. Thorium is also usually reported as "equivalent thorium" (eTh), although the thorium decay series is almost always in equilibrium.

2.17 Equilibrium and U-Series Disequilibrium.

When a radioisotope decays, producing a radioactive daughter element whose half-life is shorter than that of its parent, a condition of radioactive equilibrium will eventually be attained in which the daughter product is decaying as rapidly as it is being produced (Dewu, 1986).

The decay of U^{238} to its stable daughter, Pb^{206} and Th ^{232} to Pb ^{207} involves nineteen and eleven daughter elements respectively. If none of these daughter elements is removed out of the series, sometimes after the formation of a Uranium or Thorium bearing crystal, a state of equilibrium is reached whereby the loss of a daughter element due to its decay is made up by the decay of the proceeding parent element. This occurs where the half-life of the parent element is much larger than the half-life of the daughter element. If one of the daughter elements is taken out of the system, however, disequilibrium is established and the nuclides above the one, which has been lost become proportionally more enriched in the series. Similarly, the nuclides developed from the decay of the lost daughter elements are depleted in the series. If the nuclide, which has been lost has a short half-life then equilibrium is restored within a short time. On the other hand, the loss of nuclide with a

long half-life will mean that the series takes a long time to regain equilibrium. Due to the exponential character of radioactive decay the nuclides in a decay series approach their equilibrium values asymptotically so that 100% equilibrium is never achieved (Dewu, 1986).

In a decay series containing nuclides of varying half-lives, and where the series are headed by parents of long half-life disequilibrium between the daughter elements and their parents is better described by secular equilibrium. In this case, the daughter elements can attain 99% equilibrium with their parents and situations are usually quoted for 95% or 99% equilibrium (Dewu, 1986).

U^{238} decay series contains a number of daughter elements with very long half-lives U^{234}, Th^{230} and Ra^{226} which are members in this series, have half-lives of 4.5×10^5 Years, 8×10^6 Years and 1622 years respectively so that it will take approximately 10^6 for the U^{238} series to attain secular equilibrium. Thus, a loss of U^{234} from the series means that a period of not less than 106 years will be required before 99% equilibrium between the members in the series is restored. In the Th^{232} decay series, however, the longest lived daughter element, Ra^{232} has a half-life of just 6.7 years so that equilibrium is restored within a relatively short period of time should a member be lost from the decay series. This makes the assumption of secular equilibrium in the Th^{232} decay series safer than for the U^{238} series (Dewu, 1986).

Disequilibrium is a serious problem in the use of simple gamma ray spectrometers for U and Th determinations because both analyses are based on daughter elements which are far down the decay series. To obtain correct abundances require the existence of equilibrium

between the daughter elements and parents; Bi^{214} with U^{238} and Tl^{208} with Th^{232}. In the Th^{232} decay series, this requirement is however largely met in natural environments because of the relatively short-half lives of the members in the series the longest being Ra^{228} ($t_{1/2}$ = 6.7 years) which attain 99% equilibrium in less than 45 years (Dewu, 1986). The U^{238} series, however contains a number of very long lived daughter elements (U^{234}, Th^{230}, Ra^{226}), and a loss of any one of these will mean a longer period is needed for re-establishment of equilibrium. Of serious concern is the half-life of its gaseous daughter element, Ra^{222} ($t_{1/2}$ = 3.8 days) which is sufficiently long for it to survive to be transported to considerable distances away from its parent (Dewu, 1986).

U^{238} has also been found separated from its other daughter elements in natural environment apart from U^{238} and U^{234} fraction. Of importance in equilibrium studies are the relationship with and between Ra^{226}, Pa^{231}, Rn^{222}, Pb^{210} and Po^{210}. Whereas fractionation between U^{234} and U^{238} may be due to physical processes, fractionation between U^{238} and its other daughter is better explained by the difference in chemical properties. Radium in particular has been found to be more soluble in water than either U or Th and can thus be removed by moving water from site of its deposit. Titayeva *et al.*, (1973) reported excess Ra^{226} over Th^{230} and U^{238} in soils and sediments. This was attributed to either the deposition of Ra^{226} as adsorbed ions into clay minerals and organic matter, or preferential leaching of U^{238}. Ra^{226} is also associated with oil field brines and deposits from hot spot springs (Rosholt, 1959). Chemical fractionation preferentially enriching Pa^{231} relative to

Th^{230} in mm modules has also be reported by (Gascoyne, 1986). High Pa^{231} in high grade black, U mineral was reported by Rosolt (1959).

Rn isotopes, being gases are easily removed from members in the decay series and may be the most important because of disequilibrium in the U^{238} decay series in environments favourable to Rn diffusion. Rn is also soluble in water and can therefore, be transported in aqueous solution. Also, Rn loss can produce artificial disequilibrium during sample preparation for U analyses (Dewu, 1986).

Methods to determine the existence of equilibrium in the U decay series from gamma spectrometric data and chemical analysis have been suggested. Comparison of the results of chemical analysis and the determination of equivalent Uranium (eU) from gamma spectrometry is one of such methods (Dewu and Ahmad 1994).

2.18 Secular Equilibrium

If a radioactive nuclides decays to many daughter products to form a series such that the decay constants of the daughters are represented by λ_1, λ_2, λ_3 - - - - - - - λ_n, the activity of the nth member of the series at a time t is given by

$$C_n = -N_o\lambda_1\lambda_2 - - - \lambda_n \left[\frac{1}{(\lambda_2-\lambda_1)(\lambda_3-\lambda_1)\ldots(\lambda_n-\lambda_1)x(e^{-\lambda 1t})}\right]$$

$$- \frac{1}{(\lambda_1-\lambda_2)(\lambda_3-\lambda_{21})\ldots..(\lambda_n-\lambda_2)x(e^{-\lambda 2t})} + \text{- - - - - - - - - - -}$$

$$+ \frac{1}{(\lambda_1-\lambda_n)(\lambda_2-\lambda_n)\ldots.(\lambda_{n-1}-\lambda_n)x(e^{-\lambda nt})} \text{- - - - - - - - - - -} \quad (2.8)$$

Where N_O is the number of atoms of the parent nuclide at t = 0 (Uwah, 1984). Equation (2.8) assumes that the activity of the nth nuclide at t = 0 is zero, and also as $t \rightarrow \infty$, the activity is zero. The situation where the rate of decay of all members of a radioactive series are equal is described as secular equilibrium.

The need to assume secular equilibrium in a four channel gamma ray spectrometry is a most important drawback in the use of the method for Uranium exploration. This is because several physical and chemical factors cause disequilibrium to occur especially in the Uranium decay series as discussed above.

2.22 Previous Geophysical and Geological Research.

There is no geophysical work conducted in the study area and only one geological work but there are some relevant geophysical work conduct in other places.

Sun *et al*., (2015). Radiogenic heat production of Granitic and potential for hot dry rock geothermal resource in Guangdong province, Southern China. U^{238}, Th^{232}, and K^{40} of the granites in Guangdong. The concentration of uranium, thorium and potassium as well as density of sample taken from the study area analysed. Based on heat flow, radiogenic heat generation rate of hot dry rock potential geothermal resource in the province preliminary evaluated. Evidences shows that the province has great potential to develop HDR geothermal resources.

Olumide *et al*., (2015). Geothermal of Niger Delta Basin, Nigeria. Investigate the distribution of geothermal heat within the sedimentary fill of the Niger Delta Basin. This was achieved through the acquisition and interpretation of temperature data from the oil

wells in the region with the aim at producing geothermal maps of this Basin. Five geothermal anomalies A1, A2,A3,A4,A5,A6 centres were observed at depth in the north and north-eastern outskirts of the Niger Delta Basin as well as two A7, A8 more centres appearing at a depth of 3500m and 4000m. The background geothermal gradient value for the study area is 3^{o}/100m. At the average exploratory depth of 3500meters, the geothermal gradient values for the anomalies A1, A2, A3, A4, A5, A6, A7, and A8 are: 6.5 ˚C/100m, 1.75 ˚C/100m, 7.62 ˚C/100m, 1.25 ˚C/100m, 6.5 ˚C/100m, 5.5 ˚C/100m, 6 ˚C/100m, and 2.25 ˚C/100m respectively which means that some of them are positive and the other are negative geothermal anomalies. The study revealed that the source of the anomalies is from the basement volcanic and basic intrusion that is close to the area and migration of hot fluids from the sediments below the fault zones.

Yarima *et al*., (2013). Geothermal Energy Potential of the Chad Basin Nigeria. In which Information on geothermal gradient and heat flow within the subsurface is critical in the quest for geothermal energy exploration. In a bid to ascertain the thermal potential of Nigeria sector of the Chad Basin for energy generation, subsurface temperature information from 19 oil wells, 24 water boreholes drilled to depths beyond 100 metres and atmospheric temperature from the Chad basin were utilized in calculating geothermal gradient of the area. Selected ditch cuttings from the wells were subjected to thermal conductivity test using Thermal Conductivity Scanner (TCS) at the Polish Geological Institute Laboratory in Warsaw. The terrestrial heat flow was calculated according to the Fourier's law as a simple product of the geothermal gradient and the mean thermal conductivity. Results obtained indicated geothermal gradient range of 2.81˚C/100 m to 5.88˚C/100 m with an average of 3.71˚C/100 m. The result also indicates temperature of up to 250˚C at the top of the

basement complex, up to 85˚C at the Cenozoic unconformity, up to 200˚C at depth of 3000m b.g.l. and up to 320˚C at the depth of 5000m b.g.l. among others. The thermal conductivity values from the different representative samples range from 0.58 W/m*K to 4.207 W/m*K with an average of 1.626 W/m*K. The work presented a heat flow value ranging from 45 mW/m^2 to about 90 mW/m^2. The geothermal resources in the study area stored in the rock mass down to the deepest level (5000m) was calculated/ estimated at 1,908E+23J and this constitute an equivalent of 4.54E+15 kg of oil. The sedimentary fills of the Nigeria sector of the Chad Basin is deep enough for attainment of geothermal field, the temperature gradient and subsurface temperature are adequate for geothermal resources that might be exploited and used for some purposes.

John *et al*, (2013). Aeromagnetic and aero-radiometric data covering parts of southern Bida basin, Nigeria and the surrounding basement rocks were processed and interpreted. The research covered both basin and basement rock sections, and was aimed at determining the geothermal heat flow and radioactive heat characteristics of the survey area. The number of data points used for analysis were 2,937, obtained from the digitization of eleven ½ degrees by ½ degrees contour maps. Data processing methods used in the study include determination of heat from radiometric data, regional–residual separation of the total magnetic intensity data, determination of depth–to–top and depth–to–bottom of magnetic sources and estimation of field scaling exponent using the Fractal technique. The research results gave geothermal heat flow values ranging from 69.167 mWm^{-2} to 124.821 mWm^{-2} with an average value of 90.959 mWm^{-2} and radioactive heat values ranging from 0.91 to 4.53 $\mu W/m^3$ with an average value of 2.28 $\mu W/m^3$. Deductions made from the survey are,

the field scaling exponent varies linearly with depth of downward continuation and Katakwa is a prospect area for geothermal heat.

Garba *et al.,* (2012). Did a research work to investigate the source of Rafin Rewa and the geochemical analyses of its warm spring. They found out that it is apparent that Rafin Rewa warm water is a clear manifestation of volcanic activity, because of the nature of the water type ($NaHCO_3$) which have been classified by some authors as of volcanic origin, (Donald 1957), and also because of its high Fl content above the natural background concentration typical of the basement complex aquifers of Nigeria. Based on some criteria which include, chemical composition, relative quantity, and depth of penetration of mixing meteoric water and water of other origin Donald (1957) classified warm waters of volcanic origin as either having dominantly NaCl type and $NaHCO_3$ and or acid sulphate chloride. This also correlates with Selin *et al*., (2008) findings on the geothermal springs located along the North Anatolian Fault Zone in Turkey which are mostly Na-HCO_3 in character with the exceptions of Na-SO_4 type waters (at Yalova) and Ca-HCO_3 type waters (at Bolu and Mudurnu). But in their case the dominant HCO_3 character in the hot and the cold waters was attributed to the dissolution of reservoir rocks which are dominated by Mesozoic limestones through ion exchange with the overlying sediments which is probably responsible for the dominance of Na cation in the hot waters. But this is not the case as for the Rewa spring which is flows through crystalline metamorphic rocks (noncarbonated rocks).

Based on Donald's (1957) Classification, they concluded that the water of Rafin Rewa warm spring may have originated from the Quaternary to Recent magmatic activity that

affected the Jos Plateau area of Nigeria, and which possibly after mixing with meteoric water flows out as an ascending spring through regional lineaments that transcends the area. Belin (2012). In a preliminary survey of gamma radioactivity of some geothermal areas in the North Island of New Zealand found variation in the radio activities of soils, pools, and sinters was found between separate thermal areas, particularly between sulphate and chloride areas. In the Waiora area, the average radioactivity of hot pools with no overflow was greater than that for hot springs.

In some hot pools, the variation of gamma radioactivity with depth showed the presence of comparatively active ledges. Sinter deposits around these pools were more radioactive than nearby soils.

It is concluded that the radioactivity observed in the pools is controlled by the physical and chemical characteristics of the pools and not by the water entering from depth.

Umoren *et al*,.(2011) did a work to simulate the radioactivity of the crustal rocks of the Niger delta sedimentary basin using analytic solutions of the heat conduction equation and the method of least squares regression analysis for an earth model with radiogenic heat generation. The radiogenic heat generation capacity of the rocks was estimated using data from twenty six exploratory wells in the basin with assumption of a homogeneous earth. Radiogenic heat production per unit thermal conductivity ranged from as low as 0.0000014 to 0.004 $\mu°C\ m^2$ with mean radiogenic heat production per unit thermal conductivity of 0.0006 $\mu°Cm^2$.

Percentage radiogenic heat production calculations revealed that radiogenic heat contribution is between 0.0002 and 0.6% of the overall surface heat flow density for the Niger Delta. Mean percentage radiogenic heat production of about 0.1% was obtained.

Fraction of surface heat flow contributed by radiogenic heat generation per unit thermal conductivity was in the range of 0.0001 to 0.144 m°C m1.

Radiogenic heat production in the region was observed to be too small to have any significant effect on the thermal parameters of the region and as a result may not be included in thermal models of the basin. The low radiogenic heat generation obtained in this study agrees with the low mean heat generation values for amphibolites rocks.

Saleem *et al*., (2005) a map of radioactive heat production was constructed from airborne spectral gamma-ray data of Gebel Duwi area, Egypt. The study area possesses a range of radioactive heat production varying from 0.21 μWm^{-3} to 3.09 μWm^{-3}. Sedimentary rocks in the Gebel Duwi area have higher heat production values (0.25 μWm^{-3} to 3.09 μWm^{-3}) than the crustal average for sedimentary rocks. The average heat production of granitic rocks is below the crustal average value (1.48 μWm^{-3}) for the granites. The high values of heat production in the sedimentary rocks are mainly related to the relative increase of Uranium content in the Duwi phosphate formation. The reduced heat production of the granitic rocks indicates that additional mantle components combine with the crustal radioactive heat production to the heat sources in the Gebel Duwi area.

Omanga *et al.,* (2001) did a preliminary geophysical investigation of the source of heat of the Wikki warm spring. They showed from their results that low resistivity values exists around Wikki area. This was interpreted as an indication that the Wikki area is underlain by water. Their radiometric survey measurements revealed high gamma activity in this region, and concluded that the source of heat of the Wikki warm spring is most probably due to radioactivity.

CHAPTER THREE

MATERIALS AND METHOD

3.0 MATERIALS

Materials used in the field during the survey are as follows:

1. Digital Integral Spectral Analyser (DISA 300) gamma ray spectrometer.
2. Geographical Positioning System (GPS).
3. Measuring Tape (100m) Long.
4. Hammer.
5. Pegs.
6. Digital Tools

Which can be seen in figure 3.1 in page 54.

3.1 GROUND RADIOMETRIC (GAMMA RAY SPECTROMETRY) SURVEY.

In this research, radiometric method was used by applying Gamma ray spectrometry in order to detect/ measure gamma ray emitted from radiogenic isotopes of Uranium, Thorium and Potassium from the survey site.

There are basically two radiometric survey techniques, the ground and the air-borne radiometric surveys. The air-borne radiometric survey known as aero-radiometric survey is conducted/ applied in circumstances where the terrain is not easily accessible and/ or large areas to be prospected/covered. The technique becomes particularly advantageous because other geophysical techniques can be carried out simultaneously. The aero-surveys are superior to ground surveys for regional reconnaissance work because large areas can be covered in a relatively short time, but there is always the danger of missing important targets. There are numerous documented cases of anomalies that were missed by air borne survey owing to too wide a flight line spacing compared to the width of the anomalous

body or rugged terrain which could have prevented the aircraft from maintaining a satisfactory ground clearance (Reedman, 1979). Also, signal attenuation is worse in aero-radiometric survey than in ground radiometric survey. For example a Uranium deposit consisting of a number of veins just produced a single large airborne anomaly whereas a ground survey with a high density of sampling points defined the individual vein sources as series of separate anomalies (Ahmed 2006).

Gamma-ray spectroscopy allows determination of concentrations of selected radioelements from which the heat being produced from radioactive decay can be calculated. This may be by counting gamma-rays produced either in a rock sample during a laboratory test or an area of land during an in-situ survey. However, the relationship between recorded gamma fluency and radio-elemental concentration in the geosphere is complex. Factors such as decay series disequilibria, topographical errors, and atmospheric influence during surveying can lead to results that are not representative of the underlying rock. The radioelements of interest for geothermal resources are potassium (K), uranium (U), and thorium (Th). Rocks of high concentrations of these radioelements can be characterised by high heat flow, and the geothermal gradient can thus be favourably enhanced. Such enhancement creates usable heat at shallower depths than would otherwise be the case, thus reducing the drilling costs of a geothermal project.

3.2 Gamma Ray Spectrometry Window

The most useful radiometric technique in the detection and assessment of the radioactive elements is the gamma ray spectrometry. The gamma ray method is unusual in that it requires the consideration of many factors. The source intensity and the source-detector geometry affect observed gamma ray rates. Environmental and other effects such as soil moisture, rainfall, vegetation, non-radioactive overburden, and the distribution of airborne

sources of radiation all affect the measured rates. Each gamma ray photon has a discreet energy, and this energy is characteristic of the source isotope. This forms the basis of gamma ray spectrometry – by measuring the energies of gamma ray photons, we can determine the source of the radiation.

Because of their long half-lives, they still exist today. Of these, potassium (^{40}K), uranium (^{238}U and ^{235}U and their daughters), and thorium (^{232}Th and its daughters) are the only radio isotopes that produce high-energy gamma rays of sufficient intensity to be used for gamma ray mapping.

There are three major categories of gamma ray spectrometry, namely, multichannel, threshold (integral) and window (Darnley, 1973).

Multichannel spectrometry involves obtaining count rates from the full spectrum in a series of discreet steps or channels. Threshold spectrometry such as the one used in this work involves summing the counts from the spectrum in a series of overlapping steps by varying the energy threshold at which counting commence. For example, threshold of 1.36, 1.66 and 2.42 MeV could be used respectively to measure the sums K + U +Th, U + Th and Th alone. "window spectrometry," which is the most commonly used in most airborne, ground surveys and laboratory analyses (Grasty, 1979) involves measuring the count rates only from portions of the spectrum encompassing the photo peaks of interest. Typical window settings adopted "window spectrometry" are shown in Table 3.1

The major component of a gamma ray spectrometer is the detector crystal. The most widely used detectors for gamma ray spectrometry especially for in-situ radiometric surveys are Thallium activated sodium Iodide crystals (NaI(Tl)) (Lovborg *et al.*, 1984). Lithium drifted germanium, Ge(Li), has better energy resolution and is the most useful

laboratory analysis where high energy resolution and low energy measurements may be required. In terms of efficiency as gamma ray detector, NaI(Tl) are better than Ge(Li) detectors. The second disadvantage of Ge(Li) as a gamma ray detectors is that it must be cooled continually even when not used, to temperature of liquid nitrogen. Hyperpure Germanium detectors (HPGe), however, have excellent resolution and are better than Ge(Li) detectors . They need to be cooled only when in use. Heath, (1969) and Smith and wollenberg, (1972) have described systems making use of Ge(Li) crystal for laboratory analyses of Uranium samples.

3.3 The detector response

Thallium-doped sodium-iodide scintillation crystals are the most common detectors used in natural radioelement mapping. These detectors modify the spectrum considerably. The main aspects of the detector response are detector efficiency, directional sensitivity, energy resolution and dead time.

Detector efficiency relates to how well the detector absorbs gamma rays. The detector energy resolution is a measure of a detector's ability to distinguish between two gamma rays of only slightly differing energy. Dead time refers to the finite time required for the spectrometer to process individual photons. Heath (1964) gives a good summary of other factors that affect the shape of the pulse amplitude spectrum, such as escape events, accidental summing, and the characteristic "Compton edge". Spectrum photopeaks have Gaussian shapes. This is mainly due to the limited energy resolution of NaI detectors (IAEA, 2003).

3.4 Source-Detector Geometry

Source thickness has a significant effect on the shape of observed spectra. With increasing source thickness there is build-up of the Compton continuum due to scattering in the sources.

The photopeaks are thus reduced relative to the Compton background. Since low-energy photons are more easily attenuated than high-energy photons, this effect is more pronounced at lower energies.

Terrestrial radiation is attenuated in the source and by material between the source and the detector. The shape of the observed spectrum depends on the amount of attenuating material between the source and the detector. With increasing attenuation, the photopeaks are reduced relative to the energy continuum. Measured spectra are thus functions of the concentration and geometry of the source, the height of the detector above the ground, the thickness of any non-radioactive overburden, and the response function of the detector (IAEA, 2003).

3.5 Environmental effects.

The amount of attenuating material between the radioactive source and the gamma ray detector affects the measured radiation. In airborne gamma ray spectrometry the height of the detector above the ground has a large effect. Ten metres of air will affect the measured radiation by about 7%. Non-radioactive overburden can significantly reduce the radiation output from the earth's surface. For example, just 2 cm of cover can reduce by 35 percent the radiation penetrating to the ground surface (IAEA 2003). Dense vegetation will have the same effect. The trunks of trees in dense forests have a collimating effect on radiation from the ground. Snow cover can significantly attenuate radiation from the ground. 10 cm of fresh snow will attenuate gamma rays as effectively as 10 m of air.

Changing temperatures and pressures can lead to a change in air density by up to 30 percent. This affects the attenuation of gamma rays to the same extent. Atmospheric radon trapped in temperature inversion layers close to the ground can adversely affect estimates of background radiation in airborne surveying. Soil moisture can be a significant source of error in gamma ray surveying. An increase in soil moisture of 10 percent will decrease the measured rate by about the same amount. Precipitation can have a large effect on uranium estimation. Daughter products of airborne radon attach themselves to dust particles in the atmosphere. The radioactive precipitation of these particles by rain can lead to apparent increases of more than 2000 percent in uranium ground concentrations (Charbonneau & Darnley, 1970). Gamma ray surveying should therefore not be carried out during rainfall or shortly thereafter. About three hours is required for the anomalous surface activity to decay away. Topographic effects can be severe for both airborne and ground surveying. Both airborne and portable gamma ray spectrometers are calibrated for a 2π surface geometry. Field estimates of the concentrations of the radioelements are thus based on the assumption of a 2π source geometry. Where there are deviations from this assumption, concentration estimates will be in error. Portable spectrometer readings taken in creek beds where there are steep banks or in road cuttings will give completely erroneous results. Similarly, airborne readings in valleys or on the crests of ridges will be in error (IAEA, 2003).

Table 3.1: Typical Window Setting of Spectrometers

Integral	K-window(K40) 1.44MeV	U-window (Bi214) 1.76/1.2MeV	Th-window (Tl208) 2.62MeV	Reference
0.40-2.82	1.36-1.56	1.66-1.86	2.42-2.82	Darnley(1973)
0.40-3.00	1.36-1.75	1.66-2.42	2.44-2.81	Duval and Schultz(1979)
		1.07-1.82		
0.41-2.81	1.37-1.57	1.66-1.86	2.41-2.81	Cameron *et al*(1976)
0.72-1.36	1.36-1.56	1.66-1.86	2.41-2.81	Grasty(1975)
0.72-1.36	1.36-1.56	1.66-1.86	2.41-2.81	Grasty (1980)
0.10-2.80	1.31-1.56	1.62-1.94	2.40-2.80	Wormald *et al* (1976)
0.41-2.81	1.37-1.56	1.66-1.86	2.43-2.80	-
0.20-3.00		1.05-1.19		
0.90-2.90	1.36-1.56	1.66-1.81	2.42-2.82	Hunting (1976)

3.6 Portable gamma ray spectrometry

Portable gamma ray spectrometry has been used since the 1960's for uranium exploration, geological mapping, geothermal exploration and environmental studies. There are well-established procedures for measurement, instrument calibration and data processing.

Ground gamma ray spectrometric survey was employed for the collection of data in this study.

3.7 Instrumentation

Portable hand-held gamma ray spectrometers are widely used in field studies. Portable threshold spectrometers have up to 100 cm^3 of NaI (Tl) crystals as detectors, and several switch-operated energy thresholds. The threshold can be set to a low energy for total count measurement, and to energies slightly below 1.46 MeV, 1.76 MeV and 2.62 MeV for K, U, and Th measurement, respectively. A reference gamma ray emitting source is used for instrument gain adjustment.

3.8 Field Measurement and Data Processing.

The major GIS softwares used to process and enhance geophysical data is the Geosoft (Oasis Montaj), surfer geophysical softwares, Global mapper.

The methodology applied involved the gridding, acquisition of different radiometric data sets, building of databases, data processing and interpretation. The databases were generated to process the acquired datasets; using Geosoft softwares for processing the radiometric data. This part presents a summary of the ground spectrometric data processing methods. These methods include the orderly editing processes, the gridding and taking away of the Earths background counts of the field.

Having obtained the spectrometric data, necessary corrections then applied so as to obtain count rates, which are in proportion to the radio-element concentration. The result could then be expressed in terms of the concentration of the radioelement measured.

The procedure for estimating concentration of the three radioelements K, U and Th depends on the type of spectrometer used.

Before the calculation of the elements concentrations, the readings have to be corrected to remove back ground count effect. Where the back ground effect is negligible, the

concentration of the element is proportional to the counts recorded from the respective channel.

For a threshold spectrometer such as the one used in this study, the relationship between the count rates and the element concentration is such that the concentration is directly proportional to the background corrected count rate (Ahmed, 1994).

3.9: Field Procedure and Interpretation

A Digital Integral Spectral Analyzer (**DISA - 300**) gamma ray spectrometer manufactured by Exploranium Corporation of Canada was used for the measurements. The spectrometer is fitted with NaI (TI) sentilation detector of 5.1cm in diameter and 5.1 cm by 26.01 cm thick giving a total volume of 103cm^3. The spectrometer threshold values were 0.1 MeV for total counts, 1.3 MeV for Potassium settings, and 1.6 MeV for Uranium settings and 2.5 MeV for Thorium settings. The detector is coupled to a high gain photomultiplier tube. Because of the temperature / drift characteristics of the photomultiplier tube, the spectrometer was calibrated every day before the start of the measurements during the course of the survey to ensure that there was no channel drift. Channel calibration was done with Co^{60} calibration source. The procedure for taking readings involved placing the spectrometer at each point and taking readings in the three channels. The instrument recorded activities in counts per second. It took an average of 15 minutes to take readings at one point. A Global Positioning System (GPS) was used to measure the latitude and longitude coordinates at each Station. The measurements were taken in orderly direction by N-S direction and Area was gridded 400 m by 400 m for effective coverage of the survey site, close spacing intervals of 20 m between points were maintained, this makes the area to have 400 stations as shown in fig (3.2).

But before taking the reading in the study area, background reading is measured at zero gamma ray emission site (either close to the study area such as in a pool or river) since these type of water body is neutralizing gamma radiation. And in this research the background reading count obtained for Potassium background K_b is 13, Uranium background U_b is 11.7 and for Thorium background Th_b is 3.7. These were deducted from the individual windows count for the three radioactive isotopes of Uranium, Thorium and Potassium at each of the measurement site as it was guided by the instrument manufacturer.

Plate 3.1: Equipment used during the survey (Spectrometer, GPS, Hammer, Measurement Tape and Peg).

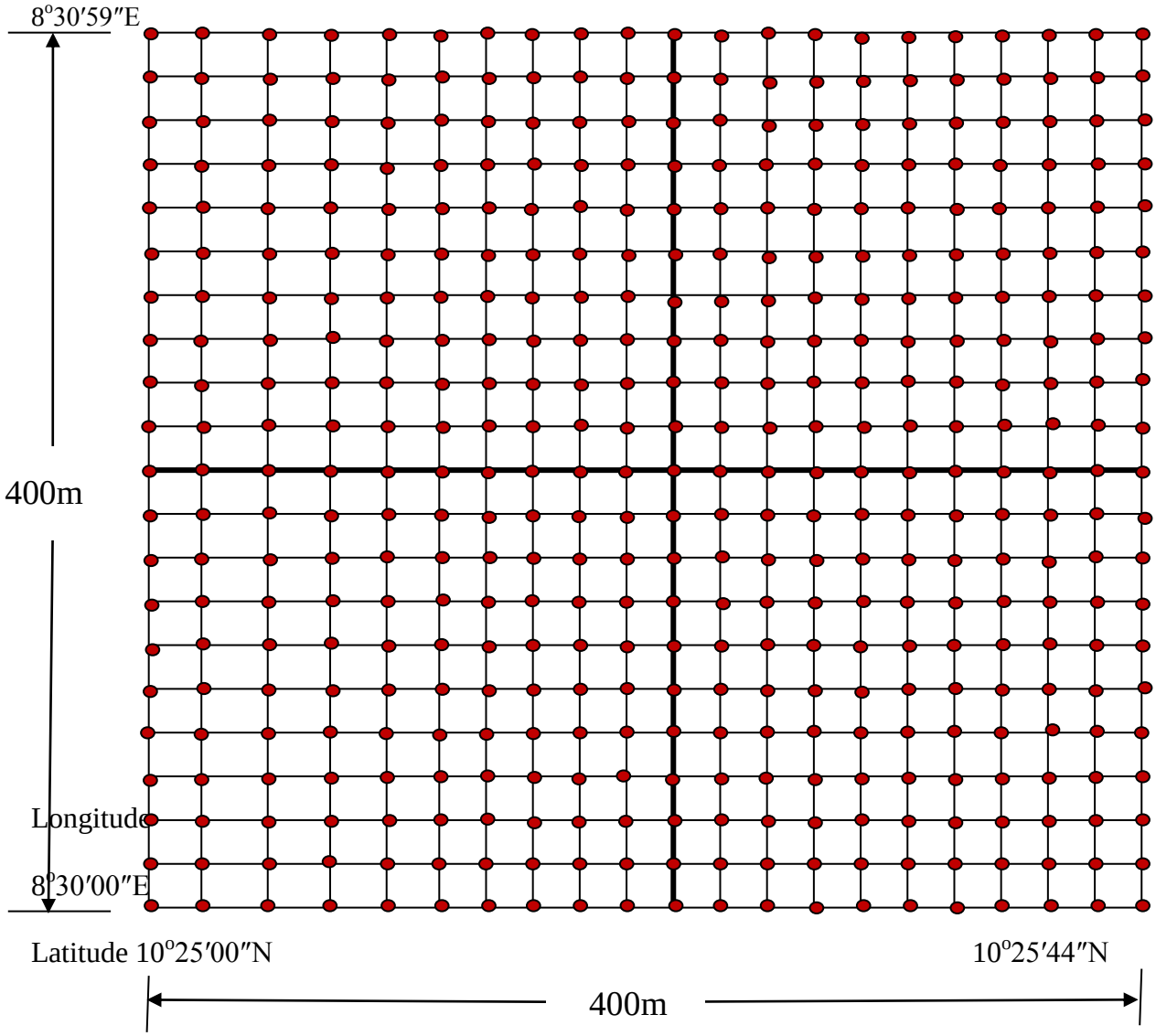

Figure 3.2 Schematic Diagram Showing the Gridded Location of the Study Area.

3.10: Radiometric Data.

Radiometric data acquired in the survey field and processed was shown in the table 3.1 below:

Table 3.1. RADIOACTIVE HEAT PRODUCED AT EACH STATION BY RADIOACTIVE ELEMENTS POTASSIUM, URANIUM AND THORIUM.

STATION NUMBERS	LONGITUDE (DEGREES)	LATITUDE (DEGREES)	POTASSIUM (K %)	URANIUM (U ppm)	THORIUM (Th ppm)	HEAT PRODUCTION HP(A) μMw^{-3}
1	10.427667	8.514472	1.167772727	79.49253659	17.29	22.54266553
2	10.427611	8.514306	0.169590909	99.00473171	17.29	27.64657342
3	10.4275	8.514139	0.147318182	74.59936585	30.59	22.09225285
4	10.427417	8.514028	0.048551948	98.8837561	123.69	35.22928413
5	10.427306	8.513861	0.211798701	50.07302439	150.29	24.14089025
6	10.427167	8.513722	0.10011039	118.4261951	97.09	38.53685253
7	10.427056	8.513583	0.175175325	152.6330244	43.89	43.84896327
8	10.426944	8.513472	0.018331169	79.46229268	43.89	24.32929013
9	10.426806	8.513306	0.074850649	20.81985366	136.99	15.37647684
10	10.426722	8.513167	0.013850649	11.1544878	57.19	7.074069077
11	10.426583	8.513028	0.043487013	6.35204878	9.31	2.364780297
12	10.426444	8.512889	0.006058442	69.57009756	163.59	30.27132674
13	10.426361	8.51275	0.146019481	30.63643902	83.79	14.18674452
14	10.426222	8.512611	0.100045455	64.72229268	136.99	27.08156597
15	10.426111	8.5125	1.167772727	79.49253659	17.29	22.54266553

3.11: Potassium (K), Thorium (Th) and Uranium (U) Channels.

By using the grid and image tools in Surfer 12 and Geosoft software (Oasis montaj), Global mapper, the count rate of radioactive elements of interest image was produced after micro-levelling the entire dataset to get rid of any apparent residual errors. These images were generated by using mini-curvature gridding since the data were collected in grid window. The images were then related with the geological units, patterns and trends.

The radioactive heat production map was developed to identify regions of both lower and higher radiogenic heat.

3.12 Data Reduction

The counts obtained from gamma spectrometric measurements had to be converted to element concentrations to be meaningful. The procedure for estimating concentration of the three radioelements K, U and Th depends on the type of spectrometer used. For a threshold spectrometer such as the one used in this work, relationship between the count rates and the element concentration in parts per million (ppm) is directly proportional to the background corrected and stripped count rate (Ahmed, 1994). The background corrected count rates were converted to relative surface element concentrations using the following conversion equations given by the instrument manufacturers (Exploranium).

eTh (ppm) $=K1\ (Thc - Thb)$ ……. (3.1)

eU (ppm) $=K2[(Uc - Ub) - S1(Thc - Thb)]$ …….. (3.2)

And K (%) $=K3[(Kc - Kb) - S2(Uc - Ub) - S3(Thc - Thb)$ …….. (3.3)

Where Thb = Average background reading in the Thorium channel

Ub = Average background reading in the Uranium channel

Kb = Average background reading in the Potassium channel

K1, K2, K3 and S1, S2, S3 are the sensitivity constants and stripping ratios for the spectrometer channels respectively. Using the constants supplied by the manufacturer, equation 3.1, 3.2, and 3.3 becomes

$$eTh\ (ppm) = 13.3*(Thc - Thb) \quad \ldots\ldots\ldots\ldots\ldots\ldots\ldots\ldots\ldots\ldots \quad (3.4)$$

$$eU\ (ppm) = \frac{200*[(Uc - Ub) - 0.62\ (Thc - Thb)]}{41} \quad \ldots\ldots\ldots\ldots \quad (3.5)$$

$$\text{And} \quad K\ (\%) = \frac{[(Kc - Kb) - 0.68\ (Uc - Ub) - 0.83\ (Thc - Thb)]}{154} \quad \ldots\ldots\ldots\ldots \quad (3.6)$$

Equation 3.4, 3.5, and 3.6 were used to estimate equivalent surface concentration eTh, eU, and K% respectively.

Once the concentration values for K %, U ppm, and Th ppm have been obtained, these values can be used to calculate the heat that is being produced by the radioactive decay in the rock (i.e., the radiogenic heat production). Radioactive Heat production (RHP) was calculated using Equation (3.7) which was developed for calculating the energy released during gamma decay of the radioelements.

According to Saleem and Fairhead, (2011) radioactive heat production (RHP) from ground gamma ray spectrometry data is given by the expression:

$$\boldsymbol{RHP\ (\mu Wm^{-3}) = \rho\ (0.0952C_u + 0.0256C_{Th} + 0.0348C_k)} \quad \textbf{- - - - - - -(3.7)}$$

(Saleem and Fairhead, 2011).

Where: RHP=radioactive heat, ρ= density of rock adapted from Telford *et al*, (1990), C_U, C_{Th}, C_K are the concentration of uranium, thorium and potassium respectively.

The eK, eU, eTh and radioactive heat production (RHP) values derived were processed using the Geosoft software (Oasis Montaj) and Surfer 12 programme software, Global mapper, for developing contours maps and ternary map.

3.13 Ternary Images.

The radioelement ternary image presents a single display of the three radioelement concentrations. This map suggests to a great extent the lithological differences due to the variations in colour. The uranium, thorium, and potassium maps emphasize regions where the specific radioelement has a total and pretty higher amount (Elawadi *et al*., 2004). Uranium (blue), Potassium (red) and Thorium (green) were represented respectively, in generating the ternary map. The maps will be discuss in Chapter four and five were generated with the relative intensities of colour to represent slight differences caused by the rock types.

CHAPTER FOUR:

RESULTS AND INTERPRETATION

4.1 Introduction

Ground radiometric datasets were used to explain the geology, and radioactive heat distribution zones in the study area. High resolution maps were created from the ground gamma ray spectrometry datasets present in the study area. On obtained the concentration of each of the radioelements Potassium (K), Uranium (U) and Thorium (Th) maps was presented below,

4.2 Potassium Concentration Distribution Map

The radioactive map (fig 4.1) below shows the concentration of K in % wt (% K) within the study area.

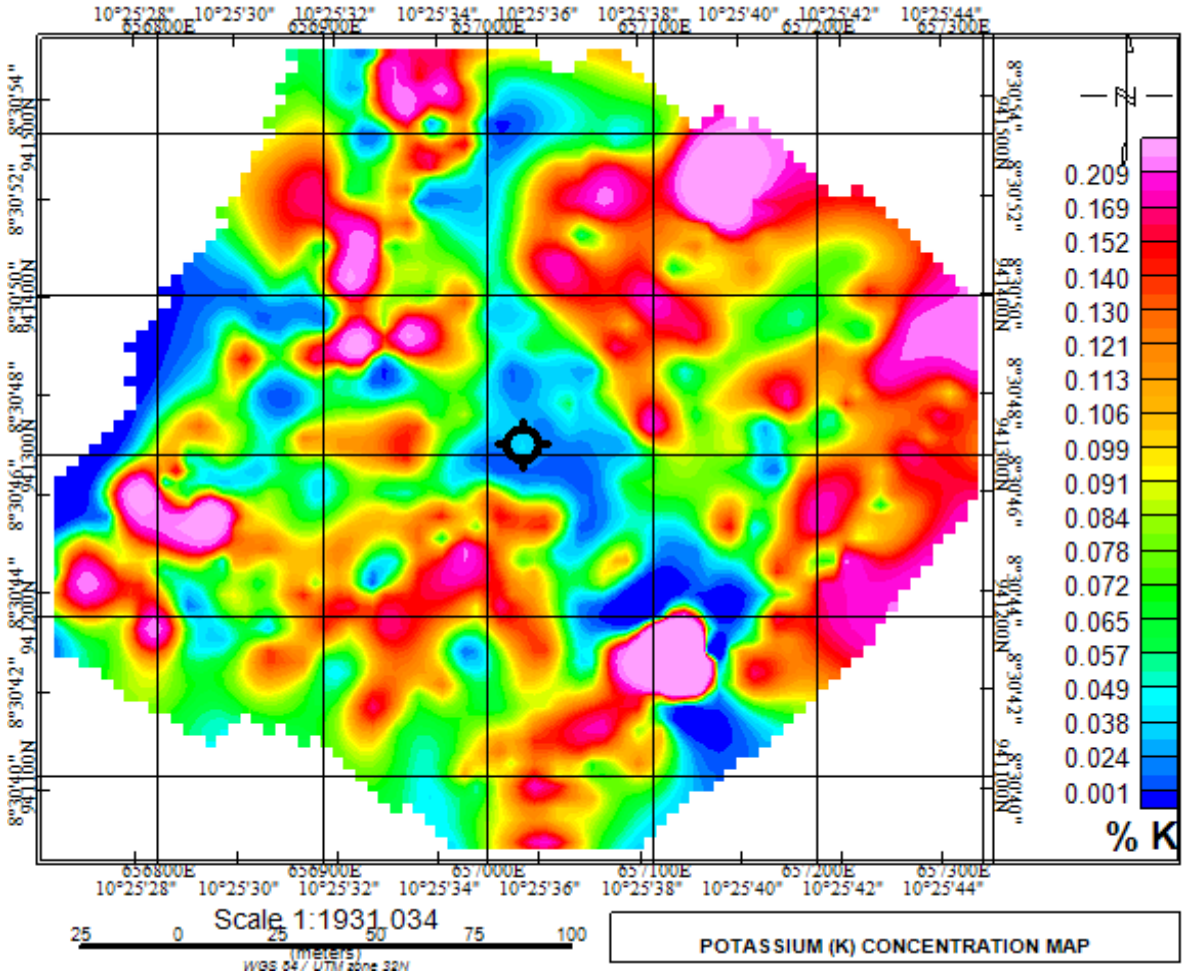

Fig 4.1: Map Showing the Concentration of Potassium (K) within the Study Area.

From Figure 4.1, areas of high and low K concentration can be seen as it was directed by the legend. From the map centre along latitude $8^0 30' 47''$ and longitude $10^0 25' 36''$ there is small black ring which is the exact manifestation of warm spring, and it was assigned black for better recognition. This map came about the black ring when the coordinates of the exact hot-spring manifestation was posted over the processed map using the same soft wares used for map processing. Areas bounded with high heat radiation from Potassium are along latitude $10^o\ 25'\ 34''$ and $10^o\ 25'\ 44''$, intersected by the longitude $8^o\ 30'\ 40''$ and $8^o\ 30'\ 54''$. While the areas with low heat distribution from this Potassium map is bounded along the coordinates latitude$10^o\ 25'\ 28''$ and $10^o\ 25'\ 34''$, and longitude $8^o\ 30'\ 42''$ and $8^o\ 30'\ 54''$

4.2 Uranium Concentration Distribution Map

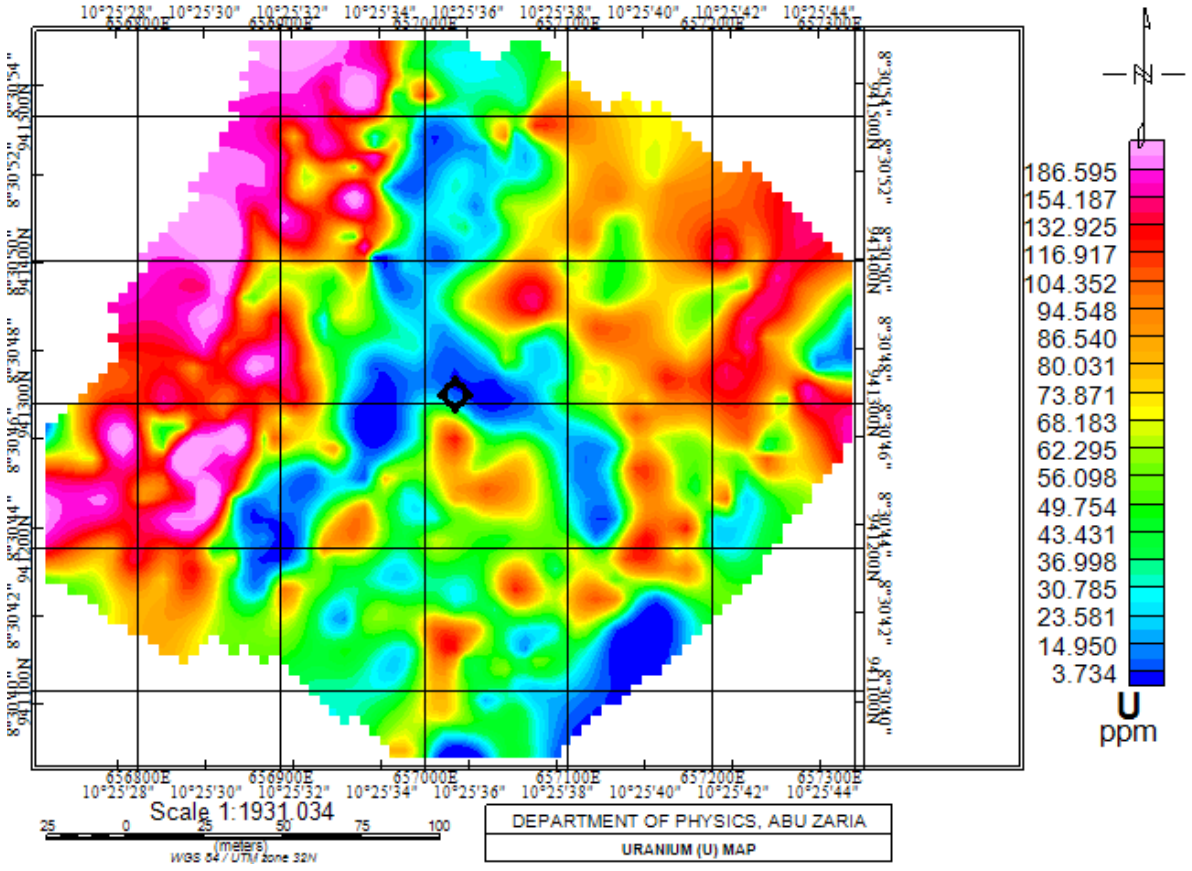

Fig. 4.2: Uranium Concentration Map of the Study area.

From figure 4.2, was able to reveal areas of high and low heat producing isotopes as it can be seen from the legend, in the map centre along latitude $8^{0}30'47''$ and longitude $10^{0}25'36''$ is small black ring is the exact manifestation of warm spring. This map came about the black ring when the coordinates of the exact hot-spring manifestation was posted over the processed map using the same soft wares used for map processing.

By looking at the map there is areas of high Uranium concentration from the anomaly along latitude 10^{o} 25′ 28″ and 10^{o} 25′ 34″ by longitude 8^{o} 30′ 44″ and 8^{o} 30′ 54″.

Still, the map was able to show areas along latitude 10^{o} 25′ 38″ - 10^{o} 25′ 44″ and longitude 8^{o} 30′ 46″ - 8^{o} 30′ 52″ were characterize with high Uranium concentration.

Again the map contain areas of low Uranium concentration, these areas are bounded along latitude 10^{o} 25′ 35″ - 10^{o} 25′ 36″ and longitude 8^{o} 30′ 44″ - 8^{o} 30′ 54″.

Furthermore, the map shows that areas bounded along 10^{o} 25′ 38″ - 10^{o} 25′ 42″ and longitude 8^{o} 30′40″ - 8^{o} 30′ 42″ are area associated with low Uranium concentration distribution.

4.3 Thorium Concentration Distribution Map

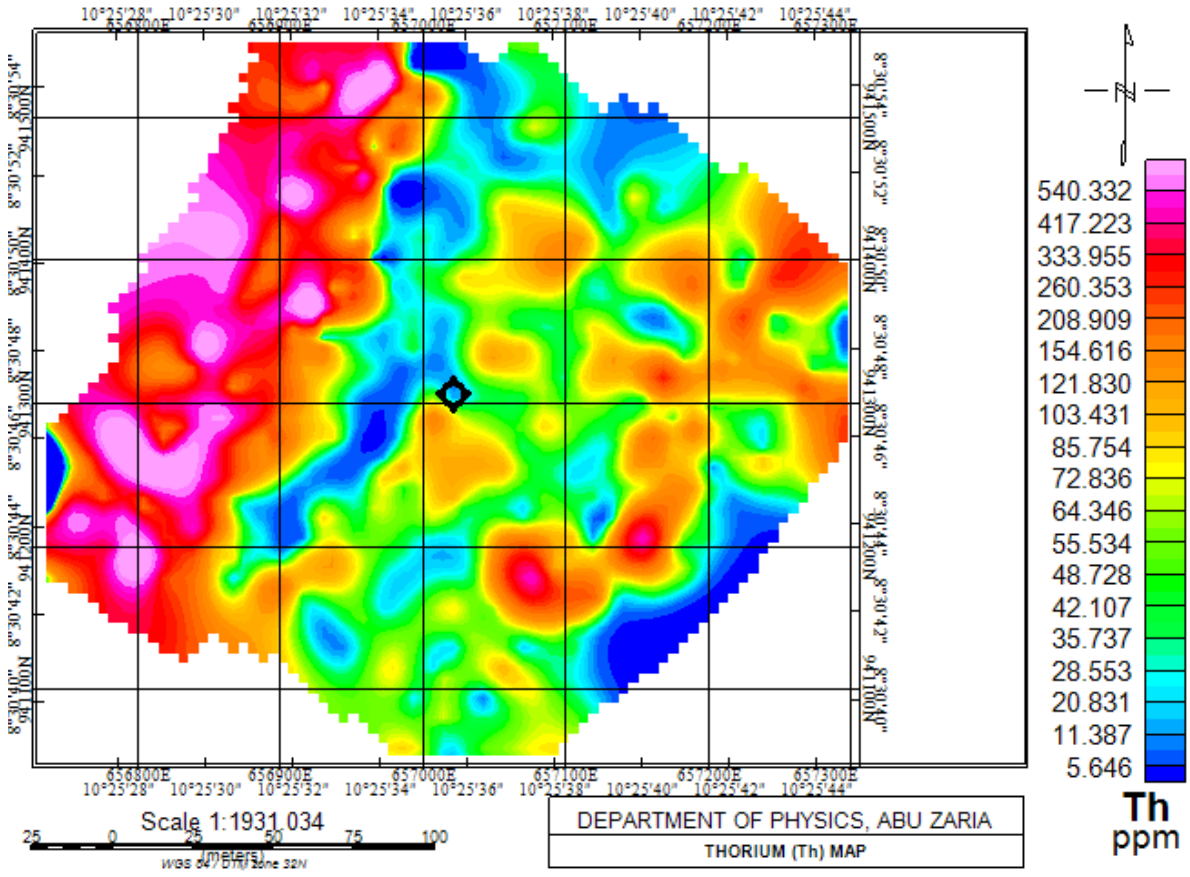

Fig. (4.3): Thorium Concentration Map of the Study area.

Fig 4.3, was able to show areas of high and low Thorium concentration distribution as it can be seen from the legend. From the map centre along latitude $8^0$30′47″ and longitude $10^0$25′36″ the small black ring at the centre of the map, shown the exact manifestation of hot-spring. This map came about the black ring when the coordinates of the exact hotspring manifestation was posted over the processed map using the same soft wares used for map processing. In the map, areas bounded along latitude 10^o 25′ 28″ - 10^o 25′ 35″ and longitude 8^o 30′ 42″- 8^o 30′ 54″ illustrated high gamma rays from Thorium concentration while at latitude 10^o 25′ 35″ - 10^o 25′ 42″ and longitude 8^o 30′ 40″ and 8^o 30′ 44″ characterized with low Thorium concentration.

4.4 Radiogenic Heat Production Map

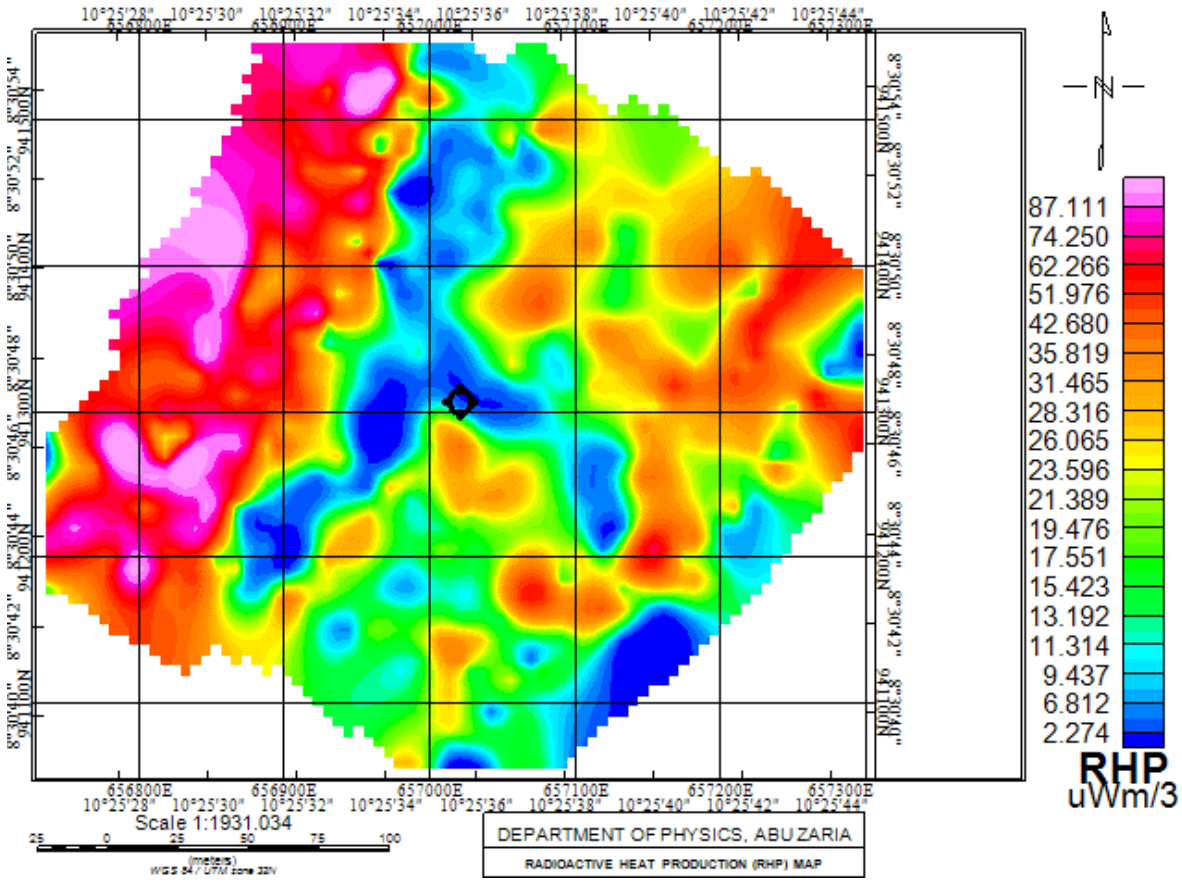

Fig 4.4: Radiogenic Heat Production Map in the Study Area.

From fig 4.4, are able to show areas of high and low radiogenic heat production within the study area. Areas bounded along latitude 10^{o} 25′ 28″ - 10^{o} 25′ 34″ and longitude 8^{o} 30′ 42″ – 8^{o} 30′ 54″ was characterized with high radiogenic heat while areas bounded along latitude 10^{o} 25′ 31″ – 10^{o} 25′ 42″ and longitude 8^{o} 30′ 40″ – 8^{o} 30′ 53″ shows low radiogenic heat production in the study area. At the centre of the map this black ring indicating location of the exact hot-spring manifestation and it was assigned to be black for better recognition on the map. This map came about the black ring when the coordinates of the exact hot-spring manifestation was posted over the processed map using the same software used for map processing.

4.5 Ternary image of the analysed data.

The table 4.1 illustrates how the various colours that appear in a ternary image can be interpreted. Red areas are high in Potassium, green areas are high in Thorium and blue areas high in Uranium. Cyan areas are high in Thorium and Uranium; magenta areas are high in Potassium and Uranium and yellow areas are high in Potassium and Thorium. White areas have high levels of all three radio-elements and black areas have low levels of all the three radio-elements of interest (U, Th and K).

Table 4.1 Preparation and Interpretation of Ternary Images of Spectrometry data (Cranfield University, UK 1990).

Radio-element	Potassium	Thorium	Uranium
Red	High	Low	Low
Green	Low	High	Low
Blue	Low	Low	High
Cyan	Low	High	High
Magenta	High	Low	High
Yellow	High	High	Low
Black	Low	Low	Low

Ternary image (Figure 4.5) are one of the most commonly used approaches for displaying and interpreting the relative intensities and interactions among the three major radio-elements (K, Th, and U) recorded by ground spectrometric surveys.

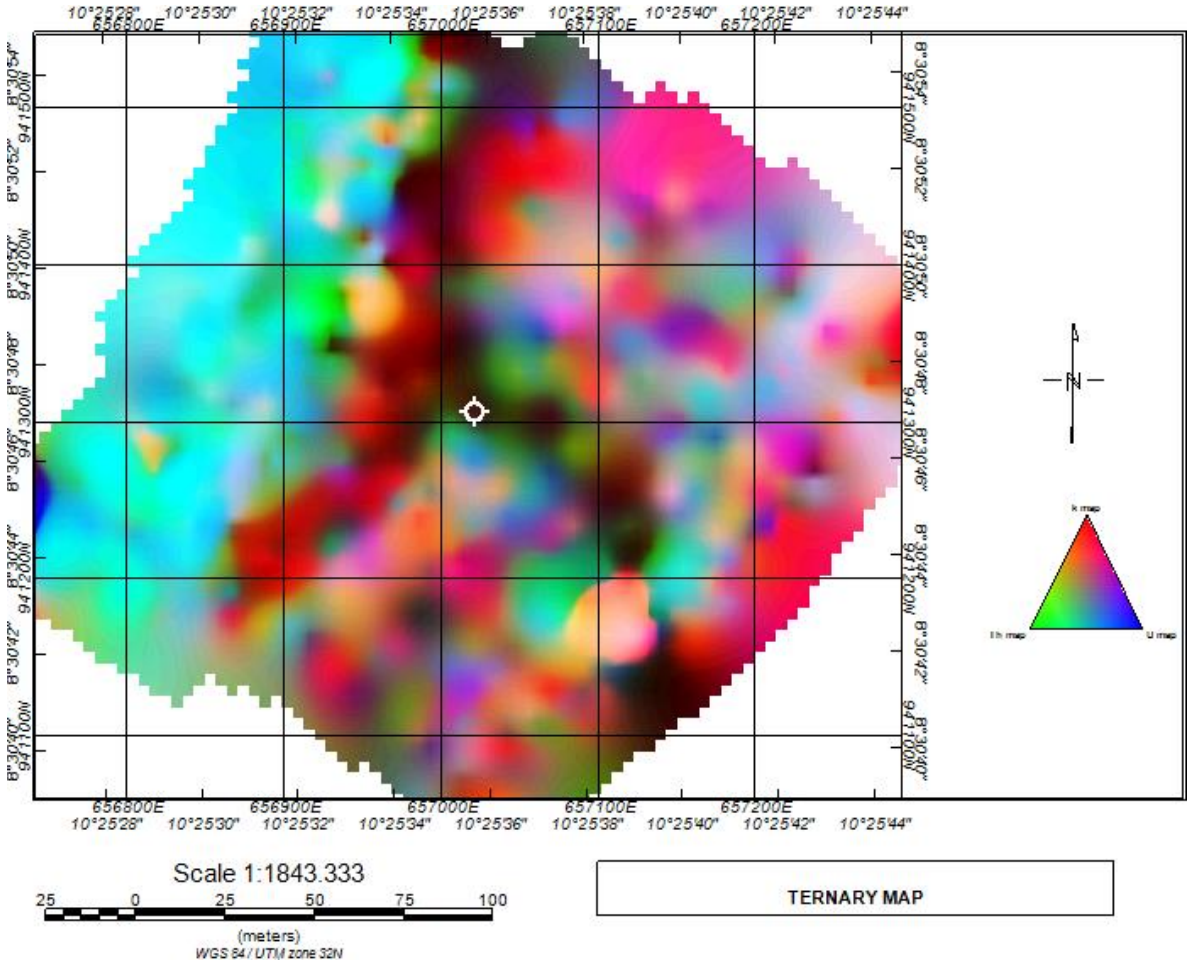

Fig 4.5 Ternary Map of the Study Area.

Fig 4.5, is the ternary image of the study area showing the concentration of all the three radioactive elements (K, U, and Th) of interest within the study area, indicating areas of high and low gamma rays concentration. The area along northwest direction along latitudes 10^0 25′ 28″-10^0 25′ 34″ and longitudes 8^0 30′ 40″-8^0 30′ 54″ reveal highest amount of concentrations of Uranium and thorium and with dotted amount concentration of Potassium from the rock and thus can be characterized by high radiogenic heat flow. At the centre of the map this white ring indicating location of the exact hot-spring manifestation and it was assigned to be white for better recognition on the map. This map came about the white ring

when the coordinates of the exact hot-spring manifestation was posted over the processed map using the same software used for map processing.

This area with high radiogenic heat flow is approximately 80 m from the hotspring manifestation.

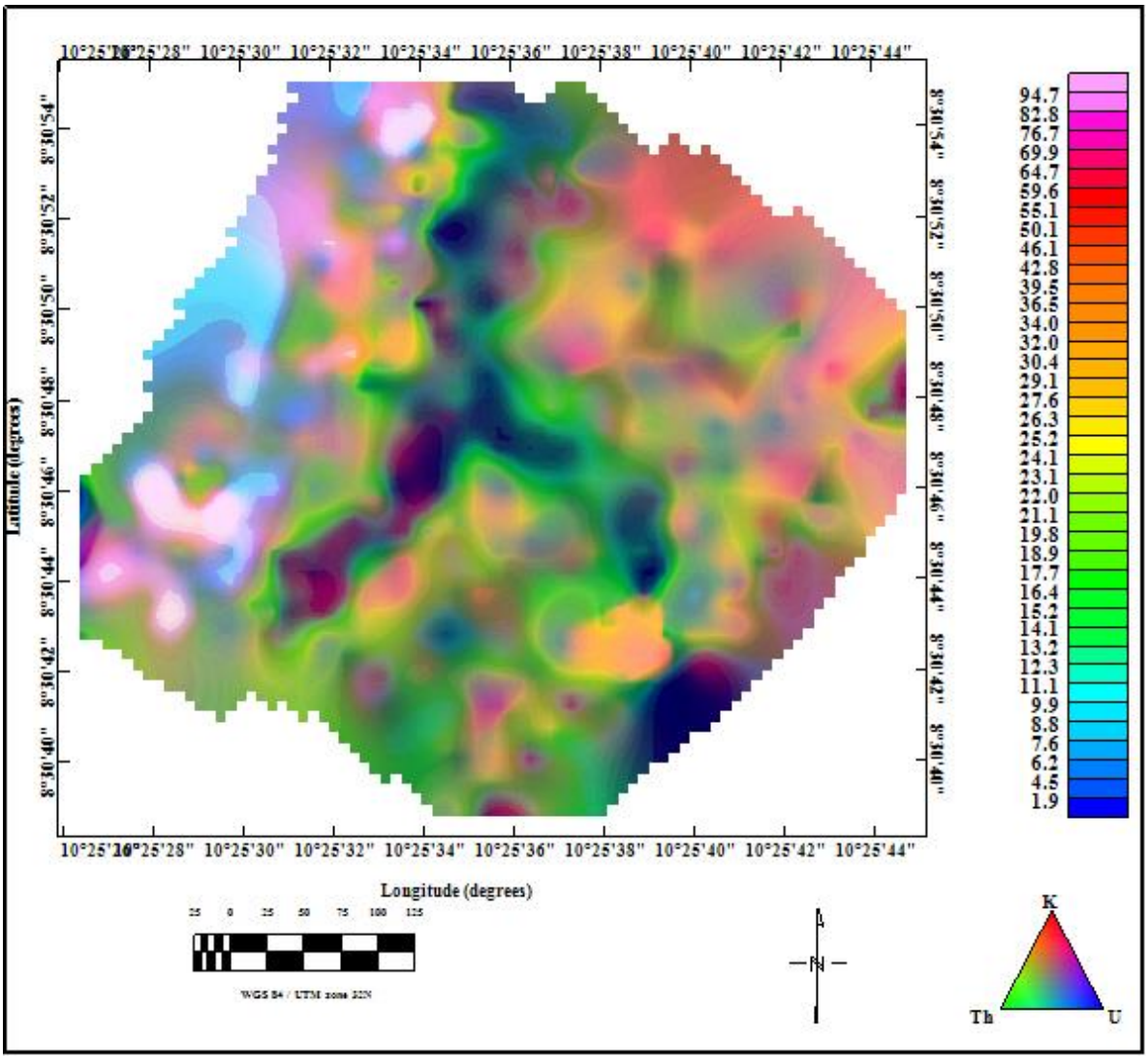

Figure 4.6: Map Showing the Correlation of RHP and Ternary Image

The map above are the correlation of RHP with Ternary image. Areas bounded along latitude 10^{o} 25′ 28″ - 10^{o} 25′ 34″ and longitude 8^{o} 30′ 42″ – 8^{o} 30′ 54″ was characterized

with high radiogenic heat and high concentration of the relative radioactive elements. Areas bounded along latitude 10^{o} 25′ 31″ – 10^{O} 25′ 42″ and longitude 8^{o} 30′ 40″ – 8^{o} 30′ 53″ shows low radiogenic heat production and low concentration of radioactive elements in the study area. It was correlated to match the radiogenic heat and relative concentrations of radioactive elements and it was concluded that northwestern part of the study area is a promising target for geothermal energy exploration.

CHAPTER FIVE

DISCUSSION

5.1 Discussions

Interpretation of potassium concentration distribution, Uranium concentration distribution, and Thorium concentration distribution; figures 4.1, 4.2 and 4.3 respectively, were done to determine areas of high concentrations of individual radioactive elements and radiogenic heat production map (Figure 4.4) and relative concentration of radioactive elements figure 4.5 ternary image for determination of radiogenic heat production and to delineate geothermal potential of the study area.

The estimated radioactive heat production values (Figures 4.4) are governed by the amount of Uranium, Thorium, and Potassium measured from ground spectrometric survey and, therefore, they are surficial or apparent values. In general, the radioactive heat production varies greatly with rock type. Any rock in the study area that indicate highest amount of radiogenic heat production from these radioelements can be characterized by high heat flow and geothermal gradient and thus can be favourably enhanced (Attia 2016). Such enhancement creates useable heat at shallower depths, thus reducing the drilling costs of a geothermal project (McCay *et al*., 2014). This explains the good correlation between the radioactive heat production map (Figure 4.4) and the geological map (Figures 1.3 and 1.4). The area possesses a range of radioactive heat production varying from 0.1552 μWm^{-3} to 154 μWm^{-3} with mean value of 31.993 μWm^{-3}. High heat-producing granites record HPR values well in excess of the global mean of 2.8 μWm^{-3} to be considered for geothermal exploration (Willmot *et* al., 2015, Vila *et al.,* 2010, Rybach, 1988). The radioactive heat production in the study area may be from the existence of migmatite gneiss since gneiss

had more of the radiation than many other rocks type (Telford *et al., 1990*) and the geology of the study area is composed of migmatite gneiss as the oldest rocks, Pan African granites and bauchites. The topography of the area is more or less flat laying with the migmatites occurring as low lying exposures, while the granitic rocks stands out conspicuously thereby dotting the landscape (Garba *et al.*, 2012). This may be attributed to the difference in the degree of metamorphism and deformation between metavolcanic and metasediments (Garba *et al.*, 2012). However, radioactive heat production may exhibit some irregularity due to the dissimilarity in the geophysical behaviour of U, Th, and K during the inspection of the analysis data of the radiogenic heat by this study produced important observation regarding the radiogenic heat production of rocks in the study area.

Firstly, for considering the first objective of this research, in Figure 4.4 the distribution of radioactive heat production cover some part of the study area but it is higher by the western part along northwest part of the map and some locations in the eastern part along northeast direction along longitude $8^0\ 30'\ 40'' - 8^0\ 30'\ 54''$ and latitude $10^0\ 25'\ 28'' - 10^0\ 25'\ 34''$.

Secondly, by mapping the area for radioactive heat production, areas with high radiogenic heat production as it can be seen from figure 4.4 the area can be delineated as a geothermal resource area. As proposed by (Attia 2016) that area of rocks containing high radiogenic heat production can be characterized as having high geothermal gradient.

Thirdly, by considering both Figure 4.4 (radioactive heat production map) and Figure 4.5 (ternary map, constructed from the three radioactive element concentrations K, U and Th) and fig.4.6 shows a strong correlation between them proving that NW direction of the study area along the longitude $8^0\ 30'\ 40'' - 8^0\ 30'\ 54''$ and latitude $10^0\ 25'\ 28'' - 10^0\ 25'\ 34''$ is a promising target and can be considered as suitable drilling target for geothermal

exploration. As it was confirmed from the work of McCay *et al*., 2014 that location of highest radiogenic heat production is a promising target for geothermal exploration (McCay *et al*., 2014).

The geology is mainly composed of migmatite gneiss and pan- African granite which dominate the lithology, this confirmed from the work of Garba *et al.,* (2012) for the origin of Rafin rewa warm spring and from the work of Saleem and fairhead, (2011) and Sun *et al*., (2016) that migmatite gneiss and granites are the reservoir rocks for radioactive element in case of geothermal investigation.

Correlation of the both the radioactive heat production map fig. 4.4 and the ternary map fig. 4.6 in fig. 4.6 indicates that north-western part of the study area was characterized with high radiogenic heat production from Uranium and Thorium as main contributing elements with highest values at 154 μWm^{-3} and mean value at 31.993 μWm^{-3} in excess of global mean value 2.8 μWm^{-3} (Willmot *et* al., 2015, Vila *et* al., 2010) respectively and can be considered as a site for geothermal project with reducing drilling costs (McCay *et al.,* 2014).

In all the interpreted maps both radioactive heat production map and ternary map the hot spring manifestation was indicated by a black triangle (in RHP) and white ring (in ternary) to enable differentiating it from other colours in the area.

This deviation of hot-spring to occur in the active radioactive zone may result from the fact that if water percolates deeply into the crust, it will be heated as it comes into contact with hot rocks (radioisotopes). As it descends through the rock, it picks up a variety of materials, everything from radium to Sulphur. Also, as it moves further the primal heat of the earth as

a result of radioactive decay. Eventually, it encounters a large thrust fault, or cracks. As water descends behind it, it forces the now heated water to ascend along the fault line to surface as hot or warm spring (Olumide *et al*., 2015).

Physics states that in an area where there is thick vegetation or pool of water radiation from radiogenic elements remain very small or near to zero due to the fact that water always dissolve gamma radiation (IAEA 2003).

CHAPTER SIX

CONCLUSION AND RECOMMENDATION

6.1 Conclusion

The interpreted ground radiometric data in this research has helped in mapping the study area around Rafin Rewa, Dan-Alhaji, Lere, Kaduna State, Nigeria. The rocks units holding the anomalies trend along the northwestern parts of the maps at longitude 8^0 30′ 40″ – 8^0 30′ 54″ and latitude 10^0 25′ 28″ – 10^0 25′ 34″ its indicates its potentiality for geothermal exploration as its rate of radiogenic heat production exceed the global mean and median value for geothermal exploration of 2.8 μWm^{-3} (Vila *et* al., 2010, sun *et al.*, 2015, Wilmot *et al., 2015* and Tamer and Walud, 2016). North-Western part of the study area can be considered as promising site for geothermal potential as it was proposed by McCay *et al.*, *(*2014) that the areas of rock with high radiogenic heat production characterized high heat flow and geothermal gradient can be enhanced favourably. For the interest to map and determine the distribution radiogenic heat production rate and its distribution along the geological structures within the study area, ground spectrometric data collected over the entire study area were processed and interpreted. The radioactive element maps were processed using microsoft office (Excel worksheet) Surfer 12 and Geosoft Oasis Montaj, and global mapper for both gridding and interpretation. Most of the delineated structures found in the area are mostly along north-western part of the Rafin Rewa.

This study attempted to provide insight on the geothermal potential around Rafin Rewa, Dan-Alhaji village area based on the data collected from ground spectrometry survey. The surveyed area possesses a range of radiogenic heat varying from 0.1552 μWm^{-3} to 154

μWm^{-3}. The average heat production granitic (migmatites gneiss) rocks in the bedrock of the area is significantly high and indicates that the north-western part of the area is suggested as an anomalous geothermal heat area. More practically, areas of high heat are increasingly being identified as possible targets for hot, dry rock geothermal resources (Hasterok *et al.*, 2011 and based on the correlation of ternary map with radioactive heat production map of the study area it was proved it is promising location for geothermal exploration. This maps also revealed that areas of high radiogenic heat production can serve as a suitable drilling target for geothermal exploration as it was confirmed from the work of Chapman *et al.*, (2011).

7.2 **Recommendation:**

Magnetic survey is highly recommended to assist in understanding the depth to the basement, Currie-depth-point and heat flow value to correlate with the result of this research for geothermal potentiality.

REFERENCES

Aero Service (1984). Final report on airborne magnetic/radiation survey in Eastern Desert,

Egypt. Work completed for the Egyptian General Petroleum Corporation (EGPC). Six volumes, Aero Service, Houston, Texas, USA.

Ahmed, A.L. (1994). Ground follow up surveys of some Radiometric Anomalies at Jingir,

Plateaustate, using gamma ray spectrometry. Unpublished M.Sc. Thesis, Ahmadu Bello University, Zaria.

Ahmed, A.L. (2006). Detailed Radiometric Surveys of The Albite Riebeckite Granites

Dutsen wai Ring Complex, Northern Nigeria. Unpublished PhD. Dissertation, Ahmadu Bello University, Zaria.

Ahmad Salem, K. Ushijima, A. Elsirafi and I. Mizunaga, (2000). Spectral Analysis of

Aeromagnetic Data for Geothermal Reconnaissance of Quesri Ara, Northem Red Sea. Egypt. Proceeding W.G.C., 4: 873- 876.

Ahmed Salem, Abouelhoda Elsirafy, Alaa Aref, Atef Ismail, Sachio Ehara and Keisuke

Ushijima, (2005). Mapping Radioactive Heat Production from Airborne Spectral Gamma-Ray Data of Gebel Duwi Area, Egypt.

Anderson D.L and G.R. Johnson,(2000). Application of the Self Potential Method to

Geothermal. Geophysics, 38 (6), 1190-1192

Annual Global Geothermal Power Production Report (2016).

Andritsos N., Dalambakis P., Arvanitis A., Papachristou M. and Fytikas M. (2015).

Geothermal developments in Greece – Country update 2010-2014, in Proceedings World Geothermal Congress 2015, Melbourne, Australia, April 19-24. Annual U.S. & Global Geothermal Power Production Report (2016).

Attia TE, Shendi EH (2016) Uranium migration history in the igneous and metamorphic rocks of Solaf-Umm Takha area, based on multi-variate statistical analysis and favorability indices, central south Sinai, Egypt. IOSR J Appl Geol Geophys (IOSR-JAGG). e-ISSN: 2321–0990, p-ISSN: 2321–0982 (Nov–Dec 2013), PP 09-20 www.iosrjournals.org

Avbovbo A. A., (1978). Geothermal Gradients in the Southern Nigerian Basin. Bulletin of Canadian Petroleum Geology. Vol.26, No.2, 268-274.

Babalola, 0.0., (2000). High-Potential Geothermal Energy Resource Areas of Nigeria and their Geological and Geophysical Assessment. American Association of Petroleum Geophysicists Bulletin, 68, 231-244.

Bandwell C.J and W.J. MacDonald, (1995). Resistivity Survey in New Zealand thermal areas. Eight Commonwealth mining and metallurgical Congress, Australia and New Zealand, New Zealand Section, 1- 7.

Bea, F., Montero, P., and Zinger, T.(2003): The Nature, Origin, and Thermal Influence of the Granite Source Layer of Central Iberia, The Journal of Geology, 111, (2003), 579-595.

Beardsmore, G.R., and Cull, J.P.(2001): Crustal Heat Flow: A Guide to Measurement and Modelling, Cambridge University Press, City (2001).

Beck, H., Lowder, W., McLaughlin, J. (1971) Insitu External Environmental Gamma-Ray Measurements Utilizing Ge (Li) and Nai (Tl) Spectrometry and Pressurized Ionization Chambers; Atomic Energy Commission: New York, NY, USA.

Bellin A.S (2012). Gamma Radioctivity in New Zealand. Energy Sector Management Assistance Program, 2012. New Funding to Boost International Support for Geothermal Energy | ESMAP [WWW Document]. World Bank Group.

Benfield, A. F. (1939). Terrestrial heat flow in Great Britain. Proc. A 173, 428-450.

Brown, G.C., and Mussett, A.E. (1993). The inaccessible Earth: An integrated view to its structure and composition (2nd ed.), Chapman and Hall, London (1993).

Bücker C. and Rybach L. (1996). A simple method to determine heat production from gamma-ray logs, Marine and Petroleum Geology 13, 373-375.

Bullard, E. C. (1965). Heat flow in South Africa. Pp. 173, 474-502.

Cameron, J.M., Charbonneau, B.W., Killeen, P.G., Carson, G.W., and Richardson, K.A. (1976). The significance of radioelement concentration measurements made by airborne gamma-ray spectrometry over the Canadian Shield; in Proceedings of International Symposium on Exploration for Uranium Deposits, proc. series, IAEA, Vienna, p. 35-54.

Cameron, G.W., Elliott, B.E., and Richardson, K.A. (1976). Effects of line spacing on contoured airborne gamma-ray spectrometry data; in Exploration for Uranium Ore Deposits, proc. series, I.A.E.A., Vienna, p. 81-92.

Chapman, D.S and Hasterok, D., (2011). Heat Production and Geotherms for the Continental Lithosphere, Earth and Planetary Science Letters, 307, (2011), 59-70.

Charbonneau B.W, and Darnley, A.G (1970). A test strip for calibration of airborne and Ground Gamma ray spectrometers. Paper 70-1B, Geological Survey of Canada.

Chopin, G. R. (1988). Humics and radionuclide migration. Radiochima Acta, 44/45: pp. 23–28.

Chiozzi, R. Pasguale, V.M. Verdoya, P. Cabella and D. Russo, (1997). Thermo physical properties of the Lapari Iavas (Southern Tyrrherian Sea). Annal Di. Genocidal, XL (6): 1493- 1503.

Darnley, A. G. (1996). Uranium exploration data and global geochemical baselines: The need for coordinated action. In Uranium Exploration Data and Techniques Applied to the Preparation of Radioelement Maps. IAEA-TECDOC-980.

Darnley, A.G., (1973). "Airborne gamma-ray survey'techniques — present and future" , Uranium Exploration Methods (Proc. Panel Vienna, 1972), IAEA, Vienna (1973)67.

Darnley, A. G., and Ford, K. L., 1989, Regional airborne gamma-ray syrvey: A review; in "Proceedings of Exploration 87: Third Decennial International Conference on Geophysical and Geochemical Exploration for Minerals and Ground Water", Geological. Survey. of Canada, Special, pp. 960 .

Dewu, B.B.M (1986). A geophysical ground follow up to an aero-radiometric anomaly at Bisichi area of Plateau state Nigeria, unpublished M.Sc. Thesis, Ahmadu Bello University, Zaria.

Dickson, B. and Scott, K. (1997). Interpretation of aerial gamma-ray surveys-adding the geochemical factors. AGSO J. Aust. Geol. Geophys. 1997, 17, 187–200.

Donald, E.W. (1957): Thermal Waters of Volcanic Origin, Geological Society of America Bulletin 1957;68;1637- 1658.doi: 10.1130/0016 7606(1957)68[1637:TWOVO]2.0.CO;2

Duval, J.S., Schultz, K.A. (1979). Calibration Constants for the Geodata International, Inc., and Texas Instruments, Inc., High Sensitivity Systems Used for the ERDA Aerial Gamma-ray Surveys, U.S. Geol. Survey, Open-File Rep. 77-159 (1979) 15.

Ehinola, O. Joshua, E., Opeloye, S. Ademola, J. (2005). Radiogenic heat production in the cretaceous sediments of Yola arm of Nigeria Benue trough: Implications for thermal history and hydrocarbon generation. Journal Applied of Science. 5, 696–701.

Elawadi E, Ammar A, and Elsirafy A (2004), Mapping surface geology using airborne gamma ray Spectrometric survey data - A case study. Proceedings of SEGJ international symposium. Nuclear Materials Authority of Egypt, Airborne Exploration Dept.

Encyclopaedia Britannica 2018.

Energy Sector Management Assistance Program, 2013. New Funding to Boost International Support for Geothermal Energy | ESMAP [WWW Document]. World Bank Group. URL https://www.esmap.org/node/3527 (accessed 2.8.16).

Erdi-Krausz, G.; Matolin, M.; Minty, B.; Nicolet, J.; Reford, W.; Schetselaar, E. (2003). Guidelines for Redioelement Mapping Using Gamma Ray Spectrometry Data; International Atomic Energy Agency: Vienna, Austria,

Evans, R.D. (1955). The Atom ic Nucleus, McGraw-Hill, New York,pp 972.

Ewa, K. And Schoeneich, K. (2010): Geothermal Exploration in Nigeria, Proceedings World Geothermal Congress 2010 Bali,Indonesia, 25-29 April.

Fertl, W. H. (1983). Gamma-ray spectral logging: a new evaluation frontier. World Oil, pp. 79–91.

Garba M.L, E. Kurowska, K. Schoeneich, I. Abdullahi (2012). Rafin Rewa Warm Spring, A New Geothermal Discovery. American International Journal of Contemporary Research Vol. 2 No. 9; September 2012.

Gascoyne J, Rollin KE. (1986). Heat Flow 8-20. In: Geothermal energy—the potential in the United Kingdom. HMSO, London. 1986; p. 8–20.

Geosoft Inc., 1996: OASIS montaj Version 4.0 User Guide, Geosoft Incorporated, Toronto.

Geosoft Inc., 1995: OASIS Airborne Radiometric Processing System Version 1.0 User's Guide, Geosoft Incorporated, Toronto.

Graham, J.D., Beauline, N.D., Sussman, D., Sadowitz, M., & Li, Y.C. (1999). Who lives near Coke? Plants and oil refineries? An exploration of the environmental inequity hypothesis. Risk Analysis, 19(2), 171-186.

Grasty R.L (1975). ”Uranium Measurement by Airborne Gamma-Ray Spectrometry.”Geophysics, 40(3), 503-519.https://doi.org/10.1190/1.1440542.

Grasty, R. (1979). Gamma ray spectrometric methods in uranium exploration—Theory and operational procedures. Geophys. Geochem. Search Met. Ores, 31, 147–155.

Grasty, R. (1980). The "field of view" of gamma-ray detectors - a discussion; Report of Activities, Part B, Geol. Surv. Can., Paper 76-1B, p. 81-82.

Hamza, V.M., and Beck, A.E (1972). Terrestial Heat Flow: The neutrino Problem of vertical Distance Heat Production in the East Alps and a Possible Energy Source in the Core, nature, 240,343-4.

Hasterok, D., and Chapman, D.S (2011). Heat Production and Geotherms for the Continental Lithosphere, Earth and Planetary Science Letters, 307, (2011), 59-70.

Heath, R.L. (1964). Scintillation spectrometry, gamma-ray spectrum catalogue 2nd cd., Vol. 1 rind 2, U.S.A.E.C. Research and Development Report 100-16880-1, Physics T.1.0.-4500 (31st ed.).

Herndon, J. M., (1979). The nickel silicide inner core of the Earth, 495-500.

Herndon, J. M. (1980). The chemical composition of the interior shells of the Earth. 149-154.

Herndon, J. M., (1982). The object at the centre of the Earth. Naturwissenschaften, 69, 34,37.

Herndon, J. M. (1998).Composition of the deep interior of the earth: divergent geophysical development with fundamentally different geophysical implications, Phys. Earth Plan. Inter., 105, 1-4.

Herndon, J. M. (2005). Scientific basis of knowledge on Earth's composition",Curr. Sci., 88(7), 1034-1037.

Herndon, J. M., (2007). Discovery of fundamental mass ratio relationships of whole-rock chondritic major elements: Implications on ordinary chondrite formation and on planet Mercury's composition, Curr. Sci., 93(3), 394-399.

Herndon, J. M. (1993). Feasibility of a nuclear fission reactor at the center of the Earth as The energy source for the geomagnetic field. J. Geomag. Geoelectr.,45, 423-437.

Herndon, J. M. (1994). Planetary and protostellar nuclear fission: Implications for planetary change, stellar ignition and dark matter. Proc. R. Soc. Lond. A455, 453-461.

Herndon, J. M., (1996). Sub-structure of the inner core of the earth. Proc. Nat. Acad. Sci. USA, 93, 646-648.

Herndon, J. M. (2003). Nuclear georeactor origin of oceanic basalt 3He/4He, evidence, and implications. Proc. Nat. Acad. Sci. USA, 100(6), 3047-3050.

Herndon, J. M. (2007). Nuclear georeactor generation of the earth's geomagnetic field. Curr. Sci.93(11), 1485-1487.

Herndon, J. M., (2006) Solar System processes underlying planetary formation, geodynamics, and the georeactor, Earth, (2006). Moon, and Planets, 99(1),53-99.

Herndon, J. M. (2005). Whole-Earth decompression dynamics. Curr. Sci., 89(10), 1937-1941.

Herndon, J. M. (2006). Energy for geodynamics: Mantle decompression thermal tsunami. Curr. Sci., 90, 1605-1606.

Herndon, J. M. (2010). Inseparability of science history and discovery. Hist. Geo Space Sci.,1, 25-41.

Hunting, P.M., (1976). Direct radiometric measurement by gamma-ray scintillation spectrometer: Parts 1 and II; Bull. Ceol. Soc. Am., v. 67, p. 395-412.

IAEA (International Atomic Energy Agency) (1991). Airborne gamma-ray spectrometer Surveying: Tech, Report. No.323. International Atomic Energy Agency.

IAEA (International Atomic Energy Agency) 1990, The use of gamma rays data to define The natural radiation Environment, Vienna.

IAEA (International Atomic Energy Agency) 2003 Guidelines for radioelement mapping using gamma ray spectrometry data, Vienna.

ICRU (1994). Gamma ray Spectrometry in the Environment, ICRU Report 53. International Commission on Radiation Units And Measurements, Bethesda, USA.

IGA (2016). Geothermal Initiative in five Andean Countries in Latin America Bochun University of Applied Sciences, Germany.

Jaupart, C. and Mareschal, J.C (2003). Constraints on crustal heat production from heat flow data. In Rudnick, R. L. Oxford (2003), 65-84.

John O.A., Ehinola, M.A. Akpanowo and O.A. Oyebanjo, (2013). Radiogenic heat production in crustal rock samples of Southeastern Nigeria. Journal of Scientific Research, 23 (2), 305-316.

Johnson D., Dennis Geist, William Chadwick, (1995). Results from new GPS and gravity monitoring networks at Fernandina and Sierra Negra Volcanoes, Gala´pagos, 2000–2002, Journal of Volcanology and Geothermal Research 150 (2006) 79 – 97.

Johnson J.M., L. Pellirin and G.W. Hohmann, (1992). Evaluation of Electromagnetic Methods for Geothermal Reservoir Detection. Geothermal Resources Council Translation, 16,241- 245.

Jessop A.M. (1990). Thermal geophysics, Elsevier , Amsterdam. Journal of Earth Sciences And Geotechnical Engineering, vol. 2, no. 2, 2012, 25-38

Keller, G.V (1981). Exploration for Geothermal Energy. In: Fitch, A.A. (Ed.). Developments in Geophysical Exploration. Method. Applied Science Publication, 107- 150.

Kellogg, L.H., Hager, B. H. and van der Hilst, R. D., (1999). Compositional stratification in the deep mantle. Science, 283, 1881-1884.

Kitzinger, P.R. (1956). Geothermal survey of hot ground near Lordsburg. New Mexico Science.124,629-630

Klaus, A. and Masson, D. G. (Eds.). College Station, Tx (Ocean Drilling program). Proc. ODP, Sci. Results, 149, 675- 682.

Kolawale, M. Lawal, John U.Megwara, Emmanuel E. Udensi, Peter I.Olasehinde, & Mohammed A. Daniyan (2013). Geothermal and radioactive heat studies of parts of southern Bida basin, Nigeria and the surrounding basement rocks.

Krishnaswami, S. (1999). Thorium encyclopedia of geochemistry, KluwerAcademic Publishers, London pp. 712.

Lachenbruch A.H and J.H. Sass, (1997). Heat flow in the United States and thermal regime of the Crust, the earth's crust, its nature and physical properties.

Langmuir, D. and Hermans, J. S. (1980). The mobility of thorium in natural waters at low Temperatures. Geochimica et Cosmochimica Acta, 44: pp. 1753–1766.

Lee Eppelbaum. (1997) Near-surface temperature survey: An independent tool for delineation of buried archaeological targets. *Journal of Cultural Heritage* **10**, e93-e103.

Lee T.C, (1977), On Shallow- hole temperature measurements. A test study in the Salton Sea Geothermal Field: Geophysics, 42, 572- 583.

Leschack L.A., and J.E. Lewis, (1983). Geothermal Prospects Surveys. Geophysics, 48 (7), 975 996.

Louden K.M, and J.C. MaresChal, (1996). Measurements of radiogenic heat production on basement samples from sites 897 and 900. In: Whitmarsh, R.B, Sawyer, D.S.,

Lovborg, L. (1984). The calibration of portable and airborne gamma-ray spectrometers— Theory, problems, and facilities. Rise Natl. Lab., 2456, 3–207.

Løvborg, L.; Bøtter-Jensen, L.; Kirkegaard, P.; Christiansen, E. (1979). Monitoring of natural soil radioactivity with portable gamma-ray spectrometers. Nucl. Instrum. Methods, 167, 341.

Lubimova, E. A., (1968): Thermal History of the Earth. The earth's crust and upper mantle, Amer.Geophys. Mon.ser 13. P. 63-77.

Marvin I., and Ramalho E., (2010). Heat flow, heat production, and lithosphere thermal regime in the Iberian Peninsula, Tectonophysics 291, 29-53.

McCay AT1, Harley TL, Younger PL, Sanderson DCW, Cresswell AJ (2014) Gamma-ray spectrometry in geothermal exploration: state of the art techniques. Energies 7:4757–4780. ISSN 1996-1073; doi:10.3390/en7084757 Merriam-webster. (2009).

Murthy, V. R., van Westernen, W.,and Fei, Y. (2003). Experimental evidence that potassium is a substantial radioactive heat source in planetary cores. Nature, 423, 163-165.

Nemzer, M. L., Carter, A., and Nemzer, K.P., (2009): Geothermal Energy.

Nwachukwu S. O., (1976). Approximate Geothermal Gradients in Niger Delta Sedimentary Basin. American Association of Petroleum Geologists Bulletin, Vol. 60, No. 7, 1073-1077.

Oladipo, A.A, E.A. Oluyemi, I.A. Tubosun, M.K. Fasisi and F.I. Ibitoye (2005). Chemical Examination of Ikogosi Warm Spring in South Western Nigeria. Journal of Applied Sciences 5 (1): 75-79.

Olatunji S. A. (1989). Geothermal gradients and temperatures of ground water in Sokoto basin, Sokoto State, Nigeria. Unpublished Master of Science thesis, Department of Geology, Ahmadu Bello University, Zaria, Nigeria.

Olumide, Adedapo Jepson, Kurowksa Ewa, Schoenick. K, Ikpokonte. A. Enoch, (2015). Geothermics of Niger Delta Basin, Nigeria. Published PhD dissertation in Hydrogeology, Department of Geology, Ahmadu Bello University, Zaria, Nigeria. International Journal of Scientific research & Engineering research, volume 4, Issue11, November-2013 39, ISSN 2229-5518.

Omanga, D.A, Abraham E., Obande Ene, Mbazor Chukwu (2001). Geophysical Investigation of Source of Heat of the Wikki Warm Spring Area. Turkish Journal of Earth Sciences. DOI: 10.3906/yer-1407-12

Onuch K. M., Ekine A. S. (1999). Subsurface temperature variation and heat flow in the Anambra Basin, Nigeria. Journal of Africal Earth Sciences, Vol. 28, No. 3, 641-652.

Oyawoye, M.O., and Makanjuola, A.A.(1972): Bauchite: a fayalite-bearing quartz monzonite. Proc. 24th LG.C.(Montreal), Sect. 2, 251-266.

Pasquale P.V and Vedoya M. (2000). Ground Radiometric Survey of U, Th, and K on Lipori Island, Italy Journal of Applied Geophysics, 38,207-217.

Pasquale P.V and M. Vedoya,(2007). Radiometric Survey for Exploration of Hydrothermal Alteration in Volcanic Sites. Journal of Geophysics, 93, 13- 20.

Preparation and Interpretation of Ternary Images of Spectrometry data (Cranfield University, UK 1990).

Philip A.O, (2005). An Introduction to Geophysical Exploration Mc Graw-Hill, New York, 70,63-89.

Physics of the Solid Earth (2015). Springer International Publishing AG Part of Springer Nature. ISSN: 1069-3513.

Pollack, H. N., Hurter, S. J. and Johnson, J. R., (1993). Heat flow from the Earth's interior: Analysis of the global data set. Rev. Geophys., 31(3), 267-280.

Rajver D. (2000). Geophysical exploration of the low enthalpy Krsko Geothermal Fields, Slovenian. Proceeding W.G.C., 1605- 1607.

Ranmingwong, J.E., Coolbaugh, M.F., Vice, G., and Edwards, M.L. (2000), "Characterizing structural controls of geothermal fields in the northwestern Great Basin: A progress report," Geothermal Resources Council Transactions, 30, 69-76.

Ray, L.; Roy, S.; Srinivasan, R. (2008). High Radiogenic Heat Production in the Kerala Khondalite Block, Southern Granulite Province, India. Int. J. Earth Sci., 97, 257–267.

Reedman K.L. (1979). Interpretation of aerial gamma ray surveys-adding the geochemical factors. AGSO Journal of Australian Geology and Geophysics,17(2): pp.187–200.

Reynolds R.L , Rosenbaun J.G, M.R. Hudson and N. S. Fishman, (1990). Rock Magnetism, the distribution of Magnetic Minerals in the Earth's Crust and Aeromagnetic anomalies In: Hanna, W.F. (Ed.). Geologic Applications of Modern Aeromagnetic Surveys: U.S. Geological. Survey Bulletin, 1924, 24- 45.

Rybach, K. R. Hokrick and W. Eugester, (1988). Vertical Earth Heat Probe Measurements and Prospects in Switzerland. Communication and Proceedings. 1, 67- 372.

Rybach, L. (1988): Determination of Heat Production Rate. In: Hänel, R., et al. (eds.) Handbook of Terrestrial Heat-Flow Determination, Kluwer Academic Publishers, Dordrecht (1988), 125-142.

Rosholt C., (1959). "Overview of geothermal surface exploration methods", Presented At Short Course VII and for Exploration Of Geothermal Resources, pp. 1-15.

Rybach L. (1976). Radioactive heat production in rocks and its relation to other petrophysical parameters, Pure & Appl. Geophysics 114, 309-318.

Rybach, L. :(1988). Determination of Heat Production Rate. *In:* Hänel, R., *et al.* (eds.) Handbook of Terrestrial Heat-Flow Determination, *Kluwer Academic Publishers*, Dordrecht (1988), 125-142.

Salem Ahmad, K. Ushijima, A. Elsirafi and I. Mizunaga, (2000). Spectral Analysis of Aeromagnetic Data for Geothermal Reconnaissance of Quesri Ara, Northem Red Sea. Egypt. Proceeding W.G.C., 4: 873- 876.

Salem Ahmed, Abouelhoda Elsirafy, Alaa Aref1, Atef Ismail, Sachio Ehara and Keisuke Ushijima (2005). Mapping Radioactive Heat Production from Airborne Spectral Gamma-Ray Data of Gebel Duwi Area, Egypt. Proceedings World Geothermal Congress 2005, Antalya, Turkey, 24-29 April 2005.

Saleem, A. & Fairhead, D. (2011). Geothermal reconnaissance of Gebel Duwl area, Northern Red Sea, Egypt using airborne magnetic and spectral gamma ray data. Getech. Pp. 1-22.

Sanderson, D.; Cresswell, A.; Scott, E.; Lang, J. (2004). Demonstrating the European capability for airborne gamma spectrometry: Results from the ECCOMAGS exercise. Radiat. Prot. Dosim, 109, 119–125.

Sandiford, D. Strobl, C., Karlsson, S., (2005). An international comparison of airborne and ground based gamma ray spectrometry. University of Glasgow UK.

Sharma, P. V, (1997): Environmental and engineering Geophysics. Cambridge University Press.

Slagstad T.M (2008). Radioactive heat production of Archean to Permian geological provinces in Norway. Norwegian J Geol 88:166–149. Trondheim 2008. ISSN 029-196X .

Smith and Wollenberg, (1972). A.R. Smith, H.A. Wollenberg : High-resolution gamma ray spectrometry for laboratory analysis of the uranium and thorium decay.

Stacey, F.D., Loper, D.E., (1988): Thermal History of the Earth: a corollary concerning non-linear Mantle rheology. Phys. Earth. Planet. Inter. 53, 167-174.

Sun Zhanxue, Andong Wang, Jinhui Liu, Baoqun Hu and Gongxin Chen (2015). Radiogenic Heat Production of Granites and Potential for Hot Dry Rock Geothermal Resource in Guangdong Province, Southern China. Proceedings World Geothermal Congress 2015 Melbourne, Australia, 19-25 April 2015.

Tamer E. Attia, and Ahmed M. Wahid (2016). Role of uranium in controlling radiogenic heat production based on gamma ray spectrometry and thermal remote sensing data, southwestern Sinai, Egypt. Environ Earth Sci (2016) 75:296 DOI 10.1007/s12665-015-5131-y.

Taylor, S.R., and McLennan, S.M. (1985). The Continental Crust: its Composition and Evolution - an Examination of the Geochemical Record Preserved in Sedimentary Rocks, Blackwell Scientific, Oxford (1985).

Telford, W.M., Geldert, L.P., Sheriff, R.E., and Keys, D.A. (1990). Applied Geophysics. Cambridge: Cambridge University Press. Second Edition.

Titayeva, G.A., and Ford, K. L., (1989), Regional airborne gamma-ray survey: A review; in "Proceedings of Exploration 87: Third Decennial International Conference on Geophysical and Geochemical Exploration for Minerals and Ground Water", Geological. Survey of Canada, Special, pp. 960.

ThinkGeo Energy, (2015). Geothermal plants supply 402 GWh or more than 50% of electricity in Kenya. Think GeoEnergy - Geotherm. Energy News.

Tripp, A.H. (1975). Geochemical techniques in exploration. Proc. 2nd UN Symp. Development and Use of Geothermal Resources 1, 53-86.

Umoren-Chad, Yehuwdah E. and Ehikuemen S. Osegbowa, (2011). Radiogenic Heat Generation in the Crustal Rocks of the Niger Delta Basin, Nigeria. Asian Journal of Earth Sciences, 4: 85-93.DOI: 10.3923/ajes.2011.85.93,
URL: https://scialert.net/abstract/?doi=ajes.2011.85.93

Ushijima K.K and W.H. Relton, (2000). 2D Inversion of VES and MT data in Geothermal Area. Proceedings W.G.C., 1909- 1914.

Uwah D.A (1984). Radioactivity for Geothermal Energy.

Uysal, T (2009): Tracing the Origin of Heat Anomalies in Hot Sedimentary Aquifer System in Australia. http://Geothermalenergy centre of Excellence .org.

Vilà .M, M. Fernández, I. and Jiménez-Munt (2010). Radiogenic heat production variability of some common lithological groups and its significance to lithospheric thermal modelling. Tectonophysics

Wedepohl, K.K (Exec. Ed) (1978), Handbook of Geochemistry, Volume 2, Part 5, Berlin, Heidelberg, New York.

Wikipedia, (2009). http://en.wikipaedia.org/wiki/wikipedia: Copyrights.

Wilford, J. R., Bierwirth, P. N., and Craig, M. A. (1997). Application of Airborne Gammaray Spectrometry in Soil/Regolith Mapping and Applied Geomorphology. AGSO Journal of Australian Geology and Geophysics, 17(2):201-216.

Willmot Noller N. M, J. S. Daly and the IRETHERM team (2015). The Contribution of Radiogenic Heat Production Studies to Hot Dry Rock Geothermal. Proceedings World Geothermal Congress 2015 Melbourne, Australia, 19-25 April 2015 Resource Exploration in Ireland.

Wordsmyth. (2010): The Premier Educational Dictionary.

World Geothermal Proceeding. (2005). World Geothermal Generation 2001-2005: State of the Art. Generation and Energy Management Division – Geothermal Production. Antalya Turkey, 24-29 April 2005.

World Geothermal Proceeding. (2015). Geothermal Power Generation in the World 2010-2014 update Report. Melbourne, Australia, 19-25 April 2015.

Wormold, M.R. and Clayton, C.G. (1976). Observations on the accuracy of gamma spectrometry in uranium prospecting; in Exploration for Uranium Ore Deposits, Proc.- Series, IAEA, Vierma, p. 149-172.

Wright, M. (1998). Nature of Geothermal Resources, in Geothermal Direct-Use Engineering and Design Guidebook, edited by John W. Lund, Geo-Heat Centre, Klamath Falls, OR, pp. 27-69.

Yerima Mohammed Kwaya, Ewa Kurowska, Abdullahi Suleiman Arabi, (2013). Geothermal Gradient and Heat Flow in the Nigeria Sector of the Chad Basin, Nigeria. Computational Water, Energy, and Environmental Engineering, 2016, 5, 70-78.http://www.scirp.org/journal/cweee
http://dx.doi.org/10.4236/cweee.2016.52007

APPENDIX

Table 4.0: RADIOACTIVE HEAT PRODUCED AT EACH STATION BY RADIOACTIVE ELEMENTS POTASSIUM, URANIUM AND THORIUM.

STATION NUMBERS	LONGITUDE (DEGREES)	LATITUDE (DEGREES)	POTASSIUM (K %)	URANIUM (U ppm)	THORIUM (Th ppm)	HEAT PRODUCTION HP(A) μwm^{-3}
1	10.427667	8.514472	1.167772727	79.49253659	17.29	22.54266553
2	10.427611	8.514306	0.169590909	99.00473171	17.29	27.64657342
3	10.4275	8.514139	0.147318182	74.59936585	30.59	22.09225285
4	10.427417	8.514028	0.048551948	98.8837561	123.69	35.22928413
5	10.427306	8.513861	0.211798701	50.07302439	150.29	24.14089025
6	10.427167	8.513722	0.10011039	118.4261951	97.09	38.53685253
7	10.427056	8.513583	0.175175325	152.6330244	43.89	43.84896327
8	10.426944	8.513472	0.018331169	79.46229268	43.89	24.32929013
9	10.426806	8.513306	0.074850649	20.81985366	136.99	15.37647684
10	10.426722	8.513167	0.013850649	11.1544878	57.19	7.074069077
11	10.426583	8.513028	0.043487013	6.35204878	9.31	2.364780297
12	10.426444	8.512889	0.006058442	69.57009756	163.59	30.27132674
13	10.426361	8.51275	0.146019481	30.63643902	83.79	14.18674452
14	10.426222	8.512611	0.100045455	64.72229268	136.99	27.08156597
15	10.426111	8.5125	1.167772727	79.49253659	17.29	22.54266553